
19 Polymer Micelles for Drug Delivery

Sungwon Kim and Kinam Park

CONTENTS

19.1 Introduction	513
19.2 Drug Solubilization Methods.....	515
19.2.1 Salt Formation	516
19.2.2 Nanosizing.....	517
19.2.3 Solubilizing Excipients	518
19.2.4 Liposomes.....	519
19.2.5 Polymer–Drug Conjugates.....	520
19.3 Polymer Micelles as a Drug Carrier	521
19.3.1 Micellar Drug Solubilization Theory	521
19.3.2 Hydrotrophy.....	524
19.3.2.1 Hydrotropes and Their Mechanism of Drug Solubilization	524
19.3.2.2 Hydrotropic Polymer Micelles	526
19.3.2.3 A Theory to Explain Hydrotrophy.....	529
19.4 Stability of Polymer Micelle.....	531
19.4.1 Stability of Polymer Micelle in Water and Buffers	531
19.4.1.1 Thermodynamic Stability	531
19.4.1.2 Kinetic Stability	533
19.4.1.3 Drug Effect	535
19.4.2 Stability of Polymer Micelle in Biological Environments.....	535
19.4.2.1 Micelle–Protein Interaction	535
19.4.2.2 PEG–Protein Interactions	536
19.4.2.3 Protein Penetration into Micelles.....	538
19.4.3 Micelle–Cell Interaction.....	538
19.4.4 <i>In Vivo</i> Stability of Polymer Micelles.....	540
19.5 Perspectives and Conclusive Remarks.....	540
References.....	543

19.1 INTRODUCTION

Polymer micelles have been used widely in the delivery of various therapeutic drugs, which are also known as active pharmaceutical ingredients (APIs). Recent advances in drug discovery technology, including an accumulated database on therapeutic targets, combinational chemistry, and high-throughput screening (HTS), have further increased the number of candidate compounds and constructed a huge pipeline for the discovery and development of new chemical entities (NCEs).^{1,2} A very large number of chemicals are hailed as new drug candidates, but almost one-third of them are poorly water soluble.³ Polymer micelles consisting of amphiphilic

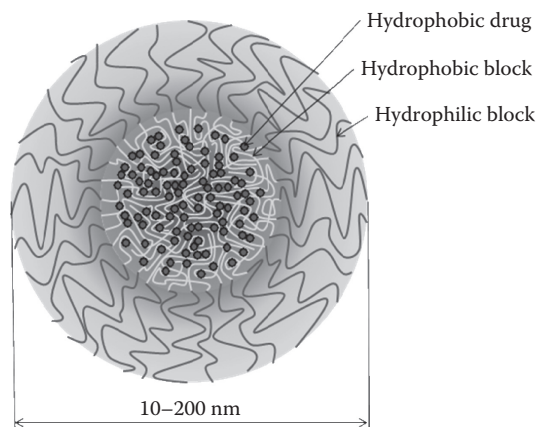


FIGURE 19.1 A typical structure of a polymer micelle in water. Amphiphilic diblock copolymers spontaneously produce a core-shell structure and lipophilic drugs are physically entrapped in the hydrophobic core. The size of a micelle is usually ranged from 10 to 200 nm.

block copolymers or lipids form a hydrophobic core, in which lipophilic drugs can be physically incorporated. Hydrophilic blocks or segments generate water-friendly corona and encapsulate the hydrophobic core. In this way, poorly soluble drugs can be successfully solubilized in aqueous media (Figure 19.1).

The size of polymer micelles loaded with hydrophobic drugs typically ranges from 10 to 200 nm in pure water. Nanosized particles dispersed in aqueous media might have a chance of intravenous (i.v.) injection. In certain inflammatory diseases, such as cancer, vascular structures become leaky, and thus, nanoparticles can extravasate into the disease site easily. This phenomenon is known as the “enhanced permeation and retention (EPR)” effect.^{4–6} During circulation in blood, nanoparticles can avoid phagocytotic clearance of the reticuloendothelial system (RES) in the spleen and the liver.^{7,8} Especially, the supramolecular structure of micelles and hydrophilic shells facilitate prolonged circulation in the bloodstream. The hydrophobic core of polymer micelles releases drug in a sustained manner, but the release pattern is tunable by controlling the hydrophobic block length and the monomer species. All those features are generally accepted as advantages of polymer micelles in drug delivery.

In spite of such advantages, only few polymer micelles are used in clinical applications. Table 19.1 lists polymer micelles used in current clinical trials. Block copolymer of monomethoxy poly(ethylene glycol) and poly(D,L-lactide) (MPEG-*b*-PDLLA) has been a popular material used to prepare polymer micelles, and is now under clinical phase I/II studies.^{9–11} MPEG-*b*-poly(aspartic acid) (PAsp) has been suggested as another possible micelle system for anticancer drug delivery, which is now in clinical phase I.^{12,13} Pluronic[®] block copolymers have been widely used in the pharmaceutical field, but only one case of clinical study has been reported.¹⁴ The first two polymers are biodegradable due to hydrolyzable ester and peptide bonds, but Pluronics are not. The chemical structures of polymers and drugs are shown in Figure 19.2.

Researchers have developed many types of micelle systems utilizing new monomers and polymers, stimuli-sensitive moieties, targeting ligands, and different therapeutic drugs. However, only a few formulations have been reported in clinical studies. Then, what are the major hurdles to developing an effective polymer micelle system that carries and delivers therapeutic drugs? The primary aim of this chapter is to answer that question. Effort will be made to discuss two important criteria: the drug loading capacity and the *in vivo* stability of polymer micelles. Polymer micelles currently under development vary in polymer topology, the nature of core-forming blocks, and the type of therapeutic drugs. This chapter focuses on diblock copolymer-based polymer micelles and their ability to solubilize hydrophobic drugs.

TABLE 19.1
Polymer Micelles in Clinical Studies

Polymer	Drug	Particle Size (nm)	Status	Maximum Tolerated Dose	References
MPEG- <i>b</i> -PDLLA (2000–1750) ^a	Paclitaxel (Genexol-PM)	30–60	Phase I/II	300 mg/m ² intravenous infusion for 3 h, once every 3 weeks	[1–3]
Pluronic L61/F127 (~2,000/~12,600)	Doxorubicin	~25	Phase I	70 mg/m ² intravenous infusion for 12.5 min, once every 3 weeks, six cycles	[4]
NK911					
MPEG- <i>b</i> -PAsp-Doxorubicin (5000–4000–543)	Doxorubicin	30–50	Phase I	67 mg/m ² intravenous infusion for 58 s –12.25 min, once every 3 weeks	[5]
NK105					
MPEG- <i>b</i> -PAsp (12,000–8,000)	Paclitaxel	~85	Phase I	180 mg/m ² intravenous infusion for 1 h, once every 3 weeks	[6,7]

Abbreviations: MPEG, methoxy poly(ethylene glycol); PDLLA, poly(D,L-lactic acid); PAsp, poly(aspartic acid).

^a Molecular weight of each block (i.e., 2000 and 1750 Da for MPEG and PDLLA, respectively).

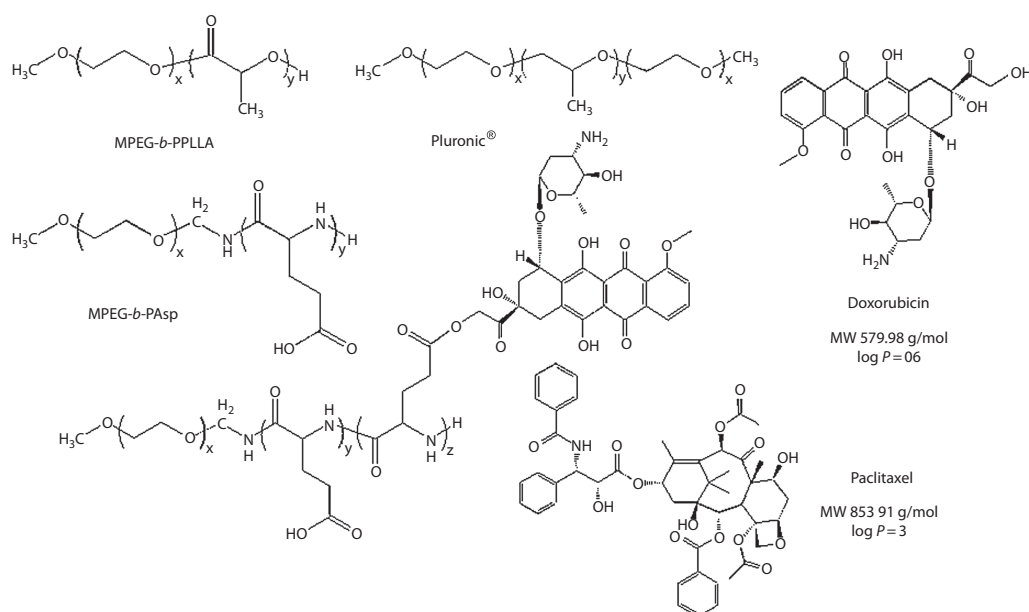


FIGURE 19.2 Structures of block copolymers and drugs examined in clinical phases. Particle size, clinical phase, and maximum tolerated dose are listed in Table 19.1.

19.2 DRUG SOLUBILIZATION METHODS

One of the primary difficulties in the formulation of pharmaceutical drugs is the poor solubility of drug candidates in water. Several methods to formulate poorly soluble drugs have been developed,

TABLE 19.2
Representative Methods to Solubilize Poorly Water-Soluble Drugs

Method	Advantages	Disadvantages
Salt formation	Simple and relatively easy formulation Applicable to protein formulation	Only drugs containing ionizable groups Common-ion effect Prone to be self-aggregated
Nanosizing	Relatively good drug stability Injectable Applicable to protein formulation	Relatively difficult to prepare Time-consuming Drug loss
Solubilizing excipient	Simple Easy and injectable formulation Applicable to protein formulation	Body toxicity Drug precipitation by dilution in body
Solid dispersion	Relatively easy Ready-to-dose form	Conditioning for good reproducibility Drug decomposition Difficult to find common solvent
Lipid emulsification	Enhancing oral adsorption Relatively easy preparation methods	Frequently low drug solubility in lipid Difficulty in lipid selection
Liposome	Injectable Versatility in surface modification Multifunctionality Applicable to protein and gene delivery	Very limited loading capacity Low carrier stability Cost of phospholipids
Polymer–drug conjugate	Injectable Versatility in backbone modification Multifunctionality Applicable to protein and gene delivery	Chemical modification of drug Only drugs with reactive side groups Purification
Polymer micelle	Injectable Versatility in monomer species Well-defined polymer structure Surface modification Multifunctionality Applicable to protein and gene delivery Relatively easy preparation method	Low loading capacity Carrier stability

but there is no standard protocol that can be applied to all drugs. Thus, development of a suitable formulation for an NCE has been a rate-limiting step in the process from drug discovery to preclinical animal studies. Failure in achieving a suitable formulation often leads to trouble with *in vitro* efficacy/safety evaluation, precipitation, poor bioavailability, and lack of dose-response proportionality after administration.¹⁵ Each formulation method for poorly soluble drugs has advantages and disadvantages as listed in Table 19.2. Understanding the basic principle and limitation of these methods is important to the development of an effective polymer micelle. In this section, representative methods for formulating poorly soluble drugs and for increasing their solubility is briefly reviewed.

19.2.1 SALT FORMATION

One of the simplest ways to increase drug solubility and dissolution rate is salt formation. It is a common, effective, and relatively easy way to increase solubility and dissolution rates of drugs with ionizable groups by the addition of counter ions. Approximately 300 drugs had been approved by Food and Drug Administration (FDA) during the period of 1995–2006, and 120 of them were in the salt form.¹⁶ Typically, solubility of a salt drug depends on the pH of media. There exists a certain

pH to achieve the maximal solubility (pH_{max}). For example, the total solubility (S_T) of a basic drug (B) is expressed by

$$\text{if } \text{pH} > \text{pH}_{\text{max}}, \quad S_T = [B]_s(1 + 10^{\text{p}K_a - \text{pH}}) \quad (19.1)$$

$$\text{if } \text{pH} < \text{pH}_{\text{max}}, \quad S_T = [\text{BH}^+]_s(1 + 10^{\text{pH} - \text{p}K_a}) \quad (19.2)$$

where $[B]_s$ and $[\text{BH}^+]_s$ are the solubility of the free drug and the protonated drug (salt), respectively. In Equation 19.1, the saturation species is B, while BH^+ is the saturation species in Equation 19.2. The intersection of two equations gives the pH_{max} . However, the drug solubility is highly influenced by ionic species in media (common-ion effect). At a given pH, for instance, the apparent solubility of the basic drug (K'_{sp}) in the presence of a counter ion (X^-) can be determined by

$$K'_{\text{sp}} = [\text{BH}^+]_s[X^-] \quad (19.3)$$

Equation 19.3 demonstrates that the maximal solubility of salt may decrease as the concentration of the counter ion increases. As a result, the dissolution rate of salt drug is significantly decreased by excess concentration of common ions. Another possible problem is self-aggregation due to the amphiphilic nature of the hydrophobic drug.¹⁷ The aggregation is generally provoked at the saturation point of ionic drugs near pH_{max} , which makes actual solubility unpredictable. The salt formation method, of course, is not useful for poorly soluble drugs without any ionizable group.

19.2.2 NANOSIZING

The nanosizing method, or nanocrystallization, reduces the size of drug particles down to the sub-micron scale.^{15,18} Until 2006, 14 formulations employing this method were examined in clinical studies.¹⁹ Dissolution rate of a nanosized drug follows the Nernst–Brunner equation that was refined later by Noyes and Whitney. If a perfect sink condition is accomplished, that is, the actual concentration of a drug in aqueous medium at time t (C_t) is much less than the saturation concentration (C_s), the equation is expressed by

$$C_t = \frac{D}{h} \times A \times C_s \quad (19.4)$$

where D , A , and h are the diffusion coefficient, the effective surface area, and the effective boundary layer thickness, respectively. Even though the drug solubility remains constant, increase of the surface area by size reduction facilitates drug dissolution in medium. The dissolution rate is important in bioavailability after oral administration of a drug formulation. Faster dissolution results in better bioavailability because of the limited locations of high drug permeation/absorption (window of adsorption) in the gastrointestinal tract for many drugs.¹⁵ At constant drug solubility, C_s can be increased by changing pH using the principle of salt formation, as discussed previously.

Nanosizing of a drug can be accomplished by either top-down or bottom-up methods.²⁰ Wet-milling and high-pressure homogenization technologies break microparticles down, while precipitation and crystallization build nanoparticles up from individual drug molecules. Regardless of nanosizing methods, a new surface area (ΔA) is generated. The free energy (ΔG) associated with this surface area is defined by

$$\Delta G = \gamma \cdot \Delta A \quad (19.5)$$

where γ represents the surface or interfacial tension. Because of the higher free energy with smaller drug particles, the nanosizing technology requires excipients that can reduce the interfacial tension (γ).

Advantages of nanosizing methods are the relatively good stability of drugs and the opportunity of intravenous injection with reduced toxicity.¹⁹ Therefore, selection of appropriate excipients is

important in this method to prevent nanosized drug particles from aggregation and to control the dissolution rate. Typically, hydroxypropylcellulose (HPC), hydroxypropylmethylcellulose (HPMC), polyvinylpyrrolidone (PVP), and Pluronic have been used as polymeric excipients.

important in this method to prevent nanosized drug particles from aggregation and to minimize the dissolution rate. Typically, hydroxypropylcellulose (HPC), hydroxypropylmethylcellulose (HPMC), polyvinylpyrrolidone (PVP), and Pluronic have been used as polymeric excipients, which are well summarized elsewhere.¹⁸ In addition, these methods can be applied to formulate protein drugs because no organic solvent is utilized.¹⁹ However, drug loss during the time-consuming nanosizing process cannot be avoided.

19.2.3 SOLUBILIZING EXCIPIENTS

If the free energy of a drug in solution is less than the free energy of the drug in solid state at constant pressure and temperature, the drug dissolves in an aqueous medium until it reaches the saturation solubility. The methods described above, salt formation and nanosizing, increase the free energy of the solid-state drug in order to move the equilibrium toward the solution-state drug. One problem that these methods frequently face is that the free energy of initial solids (salts or nanoparticles) is usually not maintained for a long time, because of salt dissociation or increase/decrease in the particle agglomeration/association/growth leading to increased size. An alternative technique is the use of solubilizing excipients. These excipients are designed to reduce the chemical potential of hydrophobic drugs in solution. At a given solubility, decrease in the chemical potential leads to the lowering of the free energy of a drug in solution.

In a cosolvent system composed of solvent and water, the total free energy of the system is the sum of the free energies of individual components. Accordingly, total drug solubility is the sum of the drug solubilities in the individual components of the system:

$$\log S_m = f \log S_c + (1 - f) \log S_w \quad (19.6)$$

where

S_m is the total solubility in the cosolvent system

S_c is the solubility of a drug in pure organic solvent

S_w is the solubility of a drug in pure water

f is the fraction of the organic solvent in the system²¹

The total solubility of drug is enhanced as the cosolvent fraction increases. In addition, excipients can be used as ligands to form a complex with drug or lipids to make an emulsion.

Various cosolvents (e.g., dimethyl sulfoxide (DMSO), ethanol, propylene glycol (PG), PEG, and dimethylacetamide (DMA)) and surfactants (such as Cremophor[®], Tween[®], and Solutol[®]) have been commonly used to improve the solubility of poorly soluble drugs.²² Cyclodextrin is a popular ligand, and currently, there exist eight different derivatives. Since 1976, more than 35 pharmaceutical products have been developed worldwide.²³ A representative product is Brexin[®], a formulation of piroxicam complexed β -cyclodextrin in the molar ratio of 1:2.5. Since launched by Chiesi Farmaceutici (Italy) in 1988, it has been a worldwide drug to control inflammation.²⁴ Excipients to enhance the drug solubility, however, are chemicals that may possess potential toxicity, originating²⁵ Toxicity of diethylene glycol (DEG), used to formulate sulfanilamide, an antibacterial agent, led to a tragic

AQ1

accident. For example, the mixture of Cremophor® EL and ethanol for paclitaxel formulation is known to frequently induce significant hypersensitivity, originating from the polyoxyl 35 castor oil. ^{26,27} In 1937, when more than 100 children died from kidney failure caused by the DEG. ²⁵ Cyclodextrin also shows subchronic and chronic toxicity. ^{28–30} To prevent such untoward incidents, the Center for Drug Evaluation and Research (CDER) of the FDA of the United States now requests industry to demonstrate suitable safety data on excipients for pharmaceutical formulation.

AQ2

The solid dispersion method can also be considered as a solubilization method using excipients. In solid dispersion, poorly soluble drugs are physically mixed with water-soluble carriers to form a eutectic mixture. ³¹ Because drugs are dispersed in the carrier matrix, the surface area is very large, and thus, the dissolution rate becomes very high (Equation 19.4). When the dispersed phase is molecularly dispersed in the carrier matrix, the eutectic mixture is called a “solid solution.” For example, Chawla and Bansal formulate irbesartan, an angiotensin II receptor agonist to treat hypertension, by the solid dispersion method (heating and quench cooling) using tartaric acid, mannitol, PVP, and HPMC as excipients. ³² Among them, tartaric acid and PVP showed significant enhancement in the solubility of irbesartan up to 9.5 and 7 fold, respectively. However, small molecular carriers frequently require high melting temperature, resulting in drug decomposition. To avoid the melting process, solvents are usually employed. Drug and carrier are dissolved in a common solvent together followed by evaporating the solvent. ³³ Because drugs are hydrophobic and carriers are usually hydrophilic, it is difficult to find a common solvent. Moreover, the extent of dispersion of a hydrophobic drug depends on the ratio of drug to carrier, which also determines the crystalline or amorphous state of the dispersed drug.

19.2.4 LIPOSOMES

Biomembrane is mainly composed of phospholipids that have a polar head group and long lipid chains. In water, they get assembled into a bilayer structure. For a pure lipid bilayer without any other biomolecules, interaction of a hydrophobic drug with the membrane might be governed by simple partitioning, which will be discussed later. The liposome is a kind of phospholipid bilayer with unique structure and properties. ³⁴ Spherical, nanosized structure of closed bilayer membrane can hold not only lipophilic compounds in the lipid layer but also hydrophilic drugs at the aqueous core (Figure 19.3). Since first introduced in 1964, ³⁵ liposomes have been a major tool used for drug

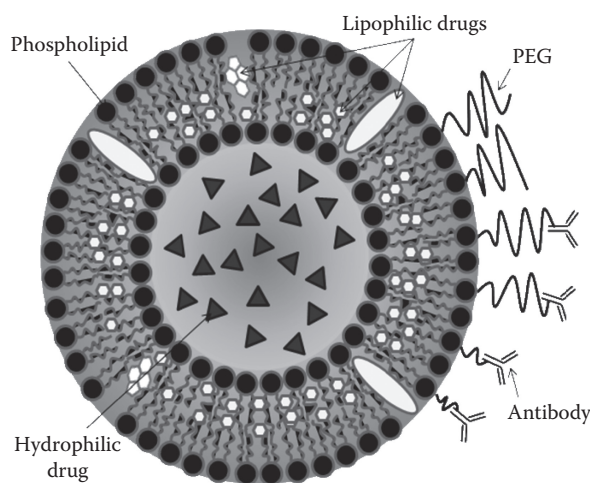


FIGURE 19.3 Representative structure of liposome. Phospholipid molecules form a bilayer in water. Lipophilic drugs are intercalated in the layer while hydrophilic drugs are encapsulated by the lipid membrane. PEG and antibodies are used to lower the RES clearance and to target liposome at specific site, respectively.

delivery. Currently there are at least 14 liposomal formulations under clinical evaluation.³⁶ The concept of drug delivery includes solubilizing poorly soluble drugs as well as delivering the drugs to a desired target site. Liposomes satisfy those requirements and also take advantages of versatility in the surface properties.^{36,37}

An early form of liposomes consisting of bare phospholipids showed opsonin- and complement-mediated clearance after intravenous administration. Liu et al. observed that liver uptake of a liposome composed of phosphatidylcholine, cholesterol, and phosphatidylserine (10:5:1) was promoted by adding serum or whole blood.³⁸ Primary parameters that influence such a clearance mechanism are the size, the surface charge, and the composition of liposomes.³⁹ Opsonization of liposomes can be significantly improved by surface modification. The size of liposomes increased by adsorption of serum proteins and opsonization, which can be mediated by the phosphatidylserine.³⁸ Cholesterols in the bilayer of a liposome interact with serum antibodies and complements resulting in blood clearance. For example, PEG conjugation increases hydrophilicity by providing prolonged circulation in blood, better biocompatibility, and reduced opsonization by RES.⁴⁰ Nevertheless, liposomes have inherent drawbacks of low blood stability, limited drug loading capacity, and expensive starting materials.

Chemical derivatives of therapeutic drugs have provided another opportunity to enhance the aqueous solubility. Such prodrugs are pharmacologically inactive compounds by themselves, but they can be converted to active forms by chemical modification after administration. Chiu et al. found that the incorporation of 15 mol% of 1,2-distearoyl-*sn*-glycero-3-phosphoethanolamine (DSPE)-PEG_{2,000} into liposomes of phosphatidylserine significantly improved the blood circulation time of the liposomes.⁴¹ In addition, targeting moieties, such as ligands or antibodies (of immunoliposomes), for an active targeting strategy is used over passive accumulation at leaky tissues by the EPR effect. Recent advances in liposome technology have brought multifunctional liposomes with multiple add-ons of stealth coating, targeting ligands, stimuli sensitivity, and imaging agents in a single carrier.⁴²

AQ3

19.2.5 POLYMER-DRUG CONJUGATES

Usually, change in the redox state,⁴³ acid-/base-catalyzed hydrolysis,^{44,45} or enzymatic metabolism evaluated trials^{46,47} are the major mechanisms to restore the drug activity. The pilot study was reported in 1975, in which Ferruti introduced a pharmacologically active polymer for the first time, called "macromolecular drug."⁴⁸ He conjugated nicotinic acid, a hydrophilicizing agent with fast excretion rate from blood, to starch backbone via hydrolyzable ester linkage; and after injection, the macromolecular drug showed good bioactivity with delayed excretion rate. Up to now, at least 13 forms of polymer-drug conjugates for cancer therapy have been evaluated in the clinical trials.^{49,50}

A representative polymer is a copolymer of *N*-(2-hydroxypropyl) methacrylamide (HPMA) and methacrylic acid. Excellent water solubility of the HPMA copolymers is good to solubilize various hydrophobic drugs, such as paclitaxel, doxorubicin, camptothecin, or palatinatate. Polymer-drug conjugates in the nanometer size take all advantages of nanomedicine, including solubility enhancement of hydrophobic drugs, prolonged blood circulation, and accumulation at leaky tissues by the EPR effect. Moreover, polymer backbone can be further modified by adding targeting ligands and imaging agents. Recent progress in genomics and proteomics has provided a unique chance to develop novel and more effective prodrugs, such as antibody-directed enzyme prodrug therapy (ADEPT) and gene-DEPT (GDEPT). Both methods aim to increase sensitivity of a target tissue (e.g., tumor) toward a prodrug. To accomplish the goal, either an enzyme directly linked to the antibody in the ADEPT or the sensitization gene in the GDEPT is injected through systematic or local administration route, followed by injecting nontoxic prodrugs. Inactive prodrugs are converted into active drugs at the desired tissue.^{46,47} However, making prodrugs requires chemical modification of APIs, causing difficulties in purification and permanent loss of drug activity. Furthermore, a prodrug is considered a new chemical entity, resulting in stringent regulatory requirements.

19.3 POLYMER MICELLES AS A DRUG CARRIER

Polymer micelles used for solubilizing poorly soluble drugs possess all advantages of other formulation methods discussed above. Amphiphilic block copolymers function as excipients to solubilize hydrophobic drugs, but polymer micelles act as drug delivery systems. Versatility in monomer species, block length ratio, and surface modification provide polymer micelles with multifunctionality. Unfortunately, however, polymer micelles have two major drawbacks: low drug loading capacity and low stability in aqueous media. This section deals with the drug loading property of polymer micelles.

19.3.1 MICELLAR DRUG SOLUBILIZATION THEORY

Hydrophobic interaction is the often cited mechanism to explain the loading of poorly water-soluble drugs in polymer micelles. The hydrophobic interaction, however, is based on the London dispersive force that occurs between all molecules. For example, aliphatic polyester blocks in an aqueous medium have a stronger London dispersive force between themselves than to polar water molecules. Likewise, the dispersive force between water molecules is much stronger than that between water and hydrophobic polymer molecules. Hydrophobic molecules become aggregated together in water to produce minimal surface contact with water molecules. Such a microscopic process looks like hydrophobic molecules hiding from water molecules. If poorly soluble drugs coexist in a polymer/water mixture system, drug molecules form aggregates with other drug molecules as well as hydrophobic polymer molecules due to their relatively stronger dispersive force toward polymers than water molecules. This, the driving force for loading a poorly soluble drug in a micelle core, is not the hydrophobic interaction, but an overall effect (hydrophobic effect) of the London dispersive force on aggregation of water-immiscible molecules in an aqueous environment. The London dispersive force is the weakest intermolecular force, but the only interaction force between nonpolar molecules. This force is based on the temporary dipole (or multipole) of nonpolar molecules and depends on the size of molecules.

In a sense, the drug loading process is a process of solubilizing drug in a polymer matrix. Therefore, it is more reasonable to explain the drug loading mechanism in terms of the solubility parameters.

Hildebrand suggested that solubility of a solute in a solvent can be expressed by the Hildebrand–Scatchard solubility parameter (δ):

$$\delta = \sqrt{\left(\frac{\Delta E_{\text{vap}}}{V}\right)} \quad (19.7)$$

where

ΔE_{vap} is the energy of vaporization
 V is the molar volume of the solvent⁵¹

The relationship was derived from Polak's equation,

$$-U = {}_r\Delta_g U + {}_g\Delta_\infty U \quad (19.8)$$

where

U is the molar internal energy
 ${}_g\Delta_g U (= \Delta E_{\text{vap}})$ is the molar vaporization energy
 ${}_g\Delta_\infty U$ is the energy required to expand the saturated vapor to infinite volume at constant temperature⁵²

In a system of nonpolar solvent, ${}_g\Delta_{\infty}U$ becomes zero ($-U = {}_g\Delta_{\infty}U$). The cohesive energy density (c) defining cohesive effect in condensed phases such as solvent is expressed by

$$c = -\frac{U}{V} \quad (19.9)$$

The Hildebrand–Scatchard solubility parameter is defined by the square root of c .^{51,52}

This model also has been a very useful method to explain the thermodynamics of polymer solutions.⁵³ The Flory–Huggins interaction parameter (χ_{12}) of two components, solvent and polymer, is defined by

$$\chi_{12} = \frac{V_1}{RT} (\delta_1 - \delta_2)^2 \quad (19.10)$$

where

V_1 is the volume of the solvent

δ_1 and δ_2 are the solubility parameters of the solvent and polymer, respectively

R is the ideal gas constant

T is the temperature

According to Equation 19.8, χ_{12} is always positive, and if $\chi_{12} < 0.5$, then the solvent is a good solvent for the polymer.

Equation 19.8, which expresses the compatibility of polymers and solvents, can be expanded to the miscibility of drugs and polymers, as follows:

$$\chi_{\text{drug-polymer}} = \frac{V_{\text{drug}}}{RT} (\delta_{\text{drug}} - \delta_{\text{polymer}})^2 \quad (19.11)$$

where

$\chi_{\text{drug-polymer}}$ is the Flory–Huggins interaction parameter between the drug and the polymer

V_{drug} is the volume of drug

δ_{drug} and δ_{polymer} are the solubility parameters of the drug and the polymer repeating unit, respectively⁵⁴

Since the Hildebrand–Scatchard solubility parameter was applied only for regular solution, an extended form of the solubility parameter, e.g., in polar solvent, was developed by Hansen.^{52,55} The Hansen solubility parameter (HSP) consists of three different interactions of dispersion (δ_d), polar (δ_p), and hydrogen bonding (δ_h) components and is expressed by

$$\delta^2 = \delta_d^2 + \delta_p^2 + \delta_h^2 \quad (19.12)$$

Each component can be calculated by following equations:

$$\delta_d = \sum \frac{F_{di}}{V} \quad (19.13)$$

$$\delta_p = \sqrt{\frac{\sum F_{pi}^2}{V}} \quad (19.14)$$

$$\delta_h = \sqrt{\left(\sum \frac{E_{hi}}{V} \right)} \quad (19.15)$$

where

- F_{di} is the molar dispersion constant
- F_{pi} is the molar dipole–dipole interaction constant
- E_{hi} is the hydrogen bonding energy
- V is the molar volume of drugs or polymers^{56,57}

Liu et al. estimated the heat of mixing (ΔH_m) between 15 homopolymers and 1 anticancer drug, ellipticine.⁵⁶ The ΔH_m can be calculated by

$$\Delta H_m = \phi_{drug} \phi_{polymer} (\delta_{drug} - \delta_{polymer})^2 \quad (19.16)$$

where ϕ_{drug} and $\phi_{polymer}$ are the volume fraction of the drug and the polymer, respectively. The dispersion, polar, and hydrogen bonding forces can be calculated from Equations 19.13 through 19.15 using the group contribution method as discussed later (Section 19.3.2.1), which leads to the total solubility parameters of drug and polymer from Equation 19.12. If they equal to zero, it means that the drug and the polymer are completely miscible. Based on the ΔH_m value of each polymer–drug pair, the solubility order of polymers with ellipticine was found to be poly(β -benzyl-L-aspartate) (PBLA_{11,500}) > poly(ϵ -caprolactone) (PCL_{14,000}) > poly(D,L-lactide) (PDLLA_{75,000–120,000}) > polyglycolide (PGA_{100,000–125,000}), where the subscript is the molecular weight (MW) of each polymer. They also evaluated the ellipticine loading efficiency of PEG₅₀₀₀-*b*-PCL₄₀₀₀ and PEG₅₀₀₀-*b*-PDLLA₄₂₀₀. The drug loading efficiency was slightly changed by the polymer-to-drug ratio, but was highly dependent on species of the micelle core-forming block. The PEG-*b*-PCL micelles loaded more than 20% (w/w) ellipticine with 76% (w/w) loading efficiency, while PEG-*b*-PDLLA micelles showed only 0.1% (w/w) loading capacity and 1.9% (w/w) loading efficiency.

In another study, Letchford et al. investigated the compatibility of five drugs (curcumin, paclitaxel, etoposide, plumbagin, and indomethacin; in the order of their aqueous solubility from low to high) with PEG₅₀₀₀-*b*-PCL₂₁₄₃ micelle.⁵⁷ The order of Flory–Huggins parameter, $\chi_{drug-polymer}$, was etoposide > paclitaxel > plumbagin > curcumin > indomethacin, which did not follow the aqueous solubility of each drug. However, the micellar drug solubilization exactly reflected the $\chi_{drug-polymer}$ values. Indomethacin showed the best solubility in micelle, while the micelle poorly solubilized etoposide. Furthermore, they determined the partition coefficient of each drug into PEG-*b*-PCL copolymers with different block lengths by the following equations:

$$\frac{[drug]_{micelle}}{[drug]_{aqueous}} = KX_{PCL} \frac{C}{\rho} \quad (19.17)$$

where

- $[drug]_{micelle}$ and $[drug]_{aqueous}$ are the concentrations of drug in micelle and water, respectively
- K is the partition coefficient of the drug
- X_{PCL} is the mole fraction of PCL in the copolymer
- C is the concentration of the copolymer
- ρ is the density of PCL

The results demonstrated that the longer PCL chain provided the better drug loading. Additionally, it was confirmed that the longer PEG chain hindered the drug partition into hydrophobic core, as they reported elsewhere.⁵⁸

The solubility and Flory–Huggins parameters can be a good index to predict the polymer–drug compatibility. By combination of Flory–Huggins theory and Hansen solubility parameters, multiple interactive forces influencing the drug loading in micelles can be explained. In addition to the dispersive intermolecular force, dipole–dipole interaction and hydrogen bonding are important in micellar drug solubilization. Lipinski also stressed the importance of hydrogen bonding to understand solubility of a drug in addition to its size and lipophilicity. From the turbidimetric aqueous solubility screening, more than half of the drugs

The solubility and Flory–Huggins parameters can be a good index to predict the polymer–drug compatibility. By combination of Flory–Huggins theory and Hansen solubility parameters, multiple interactive forces influencing the drug loading in micelles can be explained. In addition to dispersive intermolecular force, dipole–dipole interaction and hydrogen bonding are important in micellar drug solubilization.

showed poor solubility in water ($\leq 20 \mu\text{g/mL}$ in phosphate buffer, pH 7) due to the hydrogen bonding.³ The hydrogen bonding is known as a major force responsible for drug crystallization.⁵⁹ According to the theory, presence of hydrogen bonding donors and acceptors in the micelle core-forming polymer block may improve the loading capacity for drugs with hydrogen bonding moieties.

19.3.2 HYDROTROPY

19.3.2.1 Hydrotropes and Their Mechanism of Drug Solubilization

The term “hydrotropy” means the increased solubility of a lipophilic organic compound in water by the addition of large amounts of a second organic compound, hydrotrope (or hydrotropic agent).⁶⁰ The hydrotrope was first used to describe an anionic short-chain molecule that induced significant enhancement of solubility of other organic compounds in water.⁶¹ The hydrotrope has several features that are either similar to or distinct from surfactants, as listed in Table 19.3.^{61,62}

First, most hydrotropes have aromatic structure, although some of them have a linear alkyl chain. Typically, the aromatic ring is substituted by anionic or cationic side groups. Therefore, hydrotropes are amphiphiles with small MW. Some of the representative hydrotropes are shown in Figure 19.4. Second, hydrotropes are surface active, similar to surfactants, in that the surface tension of water decreases as the hydrotrope concentration increases. However, high concentration of hydrotropes is generally required to solubilize hydrophobic molecules. Also, there exists the minimal hydrotropic concentration (MHC) over which hydrotropes effectively solubilize hydrophobic compounds. While the critical micelle concentration (CMC) of a surfactant is usually a few moles, the MHC is

TABLE 19.3
Characteristic Features of Hydrotropes in Comparison to Surfactants

Difference	
Hydrotrope	Surfactant
High concentration for hydrotropic effect	Low effective concentration
Usually, aromatic structure with ionizable groups	Usually, aliphatic structure with polar head groups
Multiple mechanisms to induce hydrotropic drug solubilization (e.g., π – π stacking)	
Compound (drug) selectivity	
Similarity	
Amphiphilicity	
Surface activity	
Aggregation-induced solubilization of lipophilic molecules	

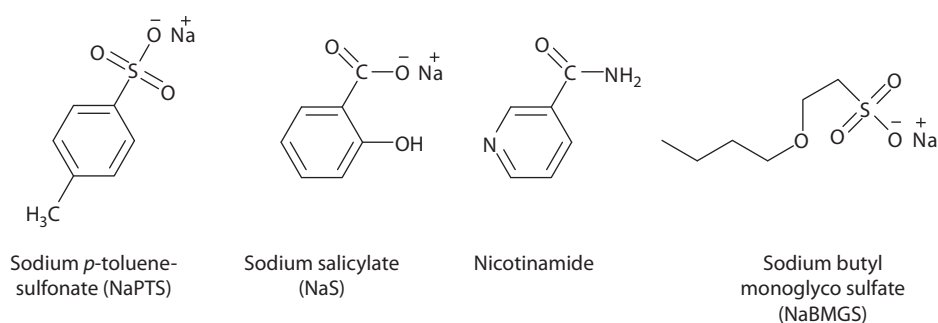


FIGURE 19.4 Structure of some hydrotropes. Typically, hydrotropes consist of an aromatic ring and a hydrophilic side group. However, some hydrotropes have a short lipid chain instead of benzene ring.

generated around 1 M.⁶³ The MHC of a certain hydrotrope is the same regardless of compounds to be solubilized, but is a specific nature depending on each hydrotrope. For instance, MHCs of sodium *p*-toluenesulfonate (NaPTS), sodium butyl monoglycol sulfate (NaBMGS), and sodium salicylate (NaS) are approximately 0.3, 0.7, and 0.8 M. However, hydrotropic effect of NaBMGS was shown at 0.7 M regardless of solutes such as fluorescein diacetate, perlyene, or ethyl *p*-nitrobenzoate.⁶⁴ The MHC can be determined by fluorospectrometry using a hydrophobic dye.⁶⁵ Third, hydrotropes more selectively solubilize hydrophobic compounds than surfactants. For example, Sanghvi et al. examined hydrotropic solubilization using nicotinamide, a famous hydrotrope, against 11 hydrophobic drugs.⁶⁶ It was found that the solubility-enhancement power of nicotinamide was not proportional to the intrinsic solubility of each drug. Furthermore, they suggested that one nicotinamide molecule formed 1:1 (drug:nicotinamide, [nicotinamide] < 10%, w/v) or 1:2 (>10%, w/v) stacking complexes with hydrophobic drugs. On the other hand, it was found that the average aggregation number of the nicotinamide for self-association was 4.37 by dynamic light scattering and vapor pressure osmometry measurements.⁶⁷ Finally, the hydrotropic activity of a hydrotrope can be improved by adding water-miscible cosolvent(s), which is called as the “facilitated hydrotropy.”⁶² For example, Simamora et al. showed that the aqueous solubility of rapamycin (in water: 2.6 $\mu\text{g}/\text{mL}$) was enhanced up to 11.26 mg/mL by mixing 5% benzyl alcohol, 10% ethanol, 40% propylene glycol, and 5% benzoate buffer.⁶⁸ The primary hydrotrope was benzyl alcohol, but its solubility in water was less than 40 mg/mL. By adding multiple cosolvents, the solubility of benzyl alcohol could be increased, which led to significant enhancement of rapamycin solubility in water. However, the facilitated hydrotropy can be induced by mixing two different hydrotropes. Evstigneev et al. found that the mixture of nicotinamide and caffeine could synergistically increase the aqueous solubility of flavin-mono-nucleotide.⁶⁹

The mechanism of hydrotropic solubilization is not clearly understood (Table 19.4). It is generally agreed that aromatic stacking is primarily attributed to the hydrotropic effect, as described above. The aromatic interaction is usually based on the charge transfer of π electrons. The sp^2 hybridized atom is composed of σ framework sandwiched by two π -electrons. The π -electron density is highly dependent on substituted heteroatoms. As shown in Figure 19.5, for example, an NH_2 -substituted ring (e.g., aniline) has more π -electrons than a NO_2 -substituted one (e.g., nitrobenzene). As a result, aniline acts as a π -electron donor while nitrobenzene is a π -electron acceptor.⁷⁰ In 1950, Mulliken suggested that charge transfer between two aromatic rings formed 1:1 complex.⁷¹ The complex generates an absorption band in the UV-VIS spectra, typically in longer wavelength region.^{70,72} However, the charge transfer band is not always observed in aromatic complexes. Therefore, charge transfer alone cannot explain the aromatic stacking phenomena. Other mechanisms for the aromatic stacking have also been suggested, which include van der Waals interaction, electrostatic interaction, induction, and desolvation.⁷³

Van der Waals force, especially London dispersive force, just like in surfactants, takes part in the hydrotropic solubilization mechanism. Several reports describe that the hydrophobic moieties

TABLE 19.4
Possible Mechanisms to Explain Hydrotropic Solubilization

Mechanism/Forces	Cases Where Typically Predominant	References
London dispersive force (hydrophobic effect)	An aromatic ring or an aliphatic chain in the structure	[8–10]
π - π stacking complex	An aromatic ring (benzene, pyridine) in the structure	[11,12]
Self-aggregation	Minimum hydrotropic concentration and stacking complexation	[11–13]
Hydrogen bonding	Hydrogen bonding donors/acceptors in the structure	[14]

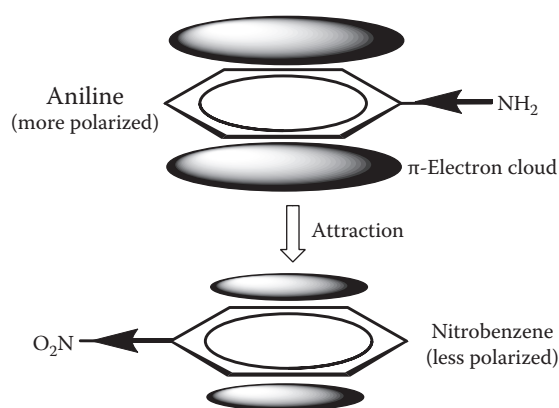


FIGURE 19.5 A simple example of π - π stacking between π -electron rich aniline and π -electron deficient nitrobenzene. Electrostatic interaction between aniline and nitrobenzene leads to stacking of both molecules.

are essential for the hydrotropic effect.^{61,63,64} Aromatic rings and aliphatic hydrocarbons are basic structures of hydrotropes. Another possible mechanism is the ionic interaction or hydrogen bonding. Heteroatoms substituting aromatic rings are mostly charged. Since hydrotropes solubilize non-electrolytes, the ionic interaction may not be a major mechanism. As described earlier, lack of hydrogen bonding is one of the important parameters responsible for the poor solubility of many drugs. Sulfonyl or carbonyl groups in hydrotropes can be hydrogen bond acceptors, while amino or hydroxyl group can be hydrogen bond donors. For example, nicotinamide, based on a pyridine ring, has an amide bond. The amide bond is not only a hydrogen bond donor, but also an acceptor, so that nicotinamide shows self-aggregation via hydrogen bonding.⁷⁴ Hydrogen bonding may not be the only force generating self-aggregates of hydrotropes, but π - π stacking as well as dispersive force also take part in producing the aggregation. Since a hydrotrope has effective solubilization effect only at concentrations over the MHC, aggregation of hydrotropes may be one of the mechanisms to explain the enhanced solubility of poorly soluble drugs. However, the aggregation is a necessary condition for hydrotropy, but not a sufficient condition. Therefore, it might be considerable that the hydrotropic solubilization power is maximized by the aggregation effect that is derived from various intermolecular interactions.

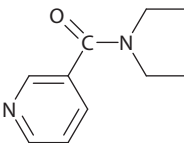
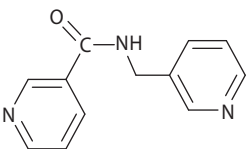
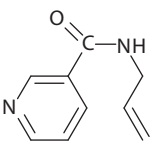
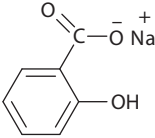
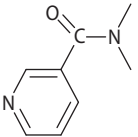
19.3.2.2 Hydrotropic Polymer Micelles

It is through the hydrotropic polymer micelle that the concept of hydrotropy was introduced to the polymer micelle. Earlier work on hydrotropic polymers was done in 2003.⁷⁵ Because a hydrotrope has selectivity in drug solubilization as described above, Lee et al. attempted to solubilize paclitaxel

as a target drug using various hydrotropes. Paclitaxel is an anticancer drug having therapeutic effect on a wide range of cancers including breast, ovarian, colon, and non-small cell lung carcinomas.⁷⁶ However, the poor solubility of paclitaxel in water has limited its use in clinical applications. Solubility enhancement power of more than 60 candidates of potential hydrotropes was initially examined.⁷⁷ The intrinsic solubility of paclitaxel was 0.3 µg/mL, and hydrotropes, mostly derivatives of nicotinamide, effectively enhanced the solubility up to the mg/mL ranges (Table 19.5).

Nicotinamide is a well-known hydrotrope to solubilize various hydrophobic drugs.^{66,78,79} With other organic compounds such as caffeine, it synergistically increases the aqueous solubility of hydrophobic solutes.^{69,80} As shown in Table 19.5, it is obvious that hydrotropic effect on paclitaxel highly depends on the structure of hydrotropes. At the concentration of 3.5 M in water, *N,N*-diethylnicotinamide (DENA) and *N*-picolylnicotinamide (PNA) enhanced the aqueous solubility of paclitaxel up to ~39 and ~29 mg/mL, respectively. However, other compounds such as NaS or *N,N*-dimethylnicotinamide (DMNA) did not achieve as much enhancement of paclitaxel solubility as DENA or PNA. It is noteworthy that the DMNA showed only ~1.8 mg/mL of drug solubility, which is much lower than that achieved by DENA.

TABLE 19.5
Some Hydrotropes Used to Solubilize Paclitaxel

Hydrotrope	Structure	Paclitaxel Solubility ^a (mg/mL)
None (pure water)		0.0003
<i>N,N</i> -Diethylnicotinamide (DENA)		39.071
<i>N</i> -Picolylnicotinamide (PNA)		29.435
<i>N</i> -Allylnicotinamide (ANA)		14.184
Sodium salicylate (NaS)		5.542
<i>N,N</i> -Dimethylnicotinamide (DMNA)		1.771

Source: Merisko-Liversidge, E.M. and Liversidge, G.G., *Toxicol. Pathol.*, 36, 43, 2008. With permission.

^a At the hydrotrope concentration of 3.5 M in water.

To prepare polymeric hydrotropes, vinyl derivatives of the PNA, 2-(2-(acryloyloxy)ethoxyethoxyethoxy)-*N*-PNA (ACEEEPNA), 2-(4-vinylbenzyloxy)-*N*-PNA (2-VBOPNA), and 6-VBOPNA were synthesized (Figure 19.6). As a result, the polymerized poly(ACEEEPNA) enhanced the aqueous solubility of paclitaxel up to 0.32 mg/mL at the hydrotrope concentration of 290 mg/mL. In addition, poly(2-(VBOPNA)) and poly(6-(VBOPNA)) retained the hydrotropic effect of PNA by increasing the paclitaxel solubility to 0.56 and 0.13 mg/mL, respectively, at the hydrotrope concentration of 165 mg/mL. Hydrotropic polymers significantly solubilized paclitaxel even at low concentrations (<50 mg/mL), in contrast to the PNA or its vinyl derivatives. Moreover, structure of PNA derivatives also influenced the solubility enhancement power even after polymerization. 2-VBOPNA with hydrophobic substitution at 2-position of pyridine ring showed the highest solubility enhancement power, while 6-substituted monomer (6-(VBOPNA)) significantly lowered the hydrotropic effect. The hydrophilic side group at the 2-position of the pyridine ring also decreased the solubility enhancement power. Structural importance of hydrotropes was also reported elsewhere.⁸¹

The hydrotropic polymer micelle was prepared from a vinyl derivative of DENA.⁸² Using a macroinitiator, brominated PEG, an amphiphilic block copolymer was synthesized from 4-(2-vinylbenzyloxy)-*N,N*-DENA (VBODENA, Figure 19.6) with a hydrophobic substitution at 4-position of pyridine ring by atom transfer radical polymerization (ATRP). It was found that PEG₅₀₀₀-*b*-poly(VBODENA)₄₃₅₀ loaded paclitaxel up to ~37% (w/w), which was much higher than the loading capacity of PEG₂₀₀₀-*b*-PLA₂₀₀₀ (~28%, w/w). Also, the paclitaxel-containing hydrotropic polymer micelle did not show any precipitation for a month when kept in water at 37°C, indicating high aqueous stability. Lee et al. confirmed the aqueous stability by measuring particle size, and reported that the hydrotropic polymer micelle had low cytotoxicity in cell culture tests.⁸³ Kim et al. suggested that the incorporation of acrylic acid moieties into the poly(VBODENA) block could modulate the drug release kinetics.⁸⁴ Because the acrylic acid moiety is hydrophilic and pH sensitive, the release profile of paclitaxel was tunable by varying the molar feed ration of VBODENA-to-acrylic acid. Introduction of more than 20% (mole) acrylic acids completely released paclitaxel within 12 h. Hydrotropic micelles containing acrylic acid did not significantly lower the paclitaxel loading capacity.

Nicotinamide is a well-known hydrotrope to solubilize various hydrophobic drugs. With other organic compounds such as caffeine, it synergistically increases aqueous solubility of hydrophobic solutes.

Another interesting feature of hydrotropic polymer micelles is the spontaneous formation of the micelle structure simply by adding a drug. It was demonstrated that a block copolymer of PEG and 2-VBOPNA successfully produced micelle structure simply by adding paclitaxel into the polymer solution.⁸⁵ Although the

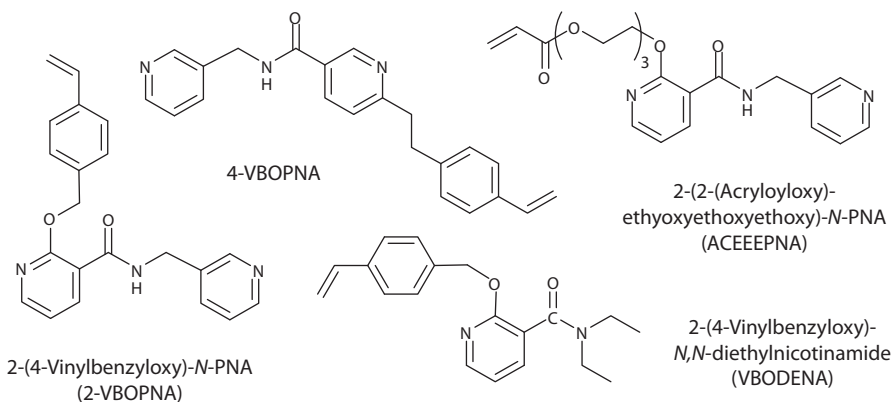


FIGURE 19.6 Hydrotropic monomers utilized for hydrotropic polymers.

hydrotropic micelle was developed to solubilize only paclitaxel, it has opened a new opportunity to improve the drug loading capacity and the aqueous stability of polymer micelles.

19.3.2.3 A Theory to Explain Hydrotropy

Conventional polymer micelles have suffered from low drug loading capacity (generally, less than 20%). However, the hydrotropic polymer micelles exhibit relatively high capacity for drug loading (up to 37%). The aqueous stability of drug-containing hydrotropic micelles was maintained for a long time. Therefore, insights into the drug loading mechanism of hydrotropic polymer micelles may suggest clues to the long-lasting questions in the field of polymer micelles—how to increase the drug loading amount and how to maintain the micelle stability after administration.

According to the theories about drug loading in polymer micelle, the maximal drug loading can be achieved by good miscibility between the drug and the polymer, as described in the previous section. However, these theories cannot fully explain the mechanism of drug solubilization by hydrotropic polymer micelles. The Flory–Huggins interaction parameter from the regular solution theory does not consider the specific interactions between drugs and polymers. Moreover, it is very difficult to obtain each component of the Hildebrand–Scatchard solubility parameter for a certain polymer. Each individual component can be calculated by the group contribution method (GCM), a kind of classical approach to predict solubility and partition coefficient.^{56,57,86} In the GCM, a mixture of two liquids is regarded as a mixture of the functional groups on each liquid. Because the GCM is based on the vapor–liquid equilibrium data, it has its limitations in predicting the polymer–drug interaction.⁸⁷

Recently, Mokrushina et al. reported a modified universal quasi-chemical functional-group activity coefficient (UNIFAC), similar to GCM, to predict the partition coefficient of organic compounds between water and micelles.⁸⁸ The classical UNIFAC model consists of two contributions: a combinatorial part responsible for the difference in molecular size and shape ($\gamma_i^{\text{combinatorial}}$), and a residual part accounting for group–group interactions ($\gamma_i^{\text{residual}}$). In the modified UNIFAC, a new contribution of the interfacial part ($\gamma_i^{\text{interfacial}}$) was introduced. As a result, the activity coefficient of the modified UNIFAC with an interfacial (IF) contribution is expressed by

$$\ln \gamma_i^{\text{UNIFAC-IF}} = \ln \gamma_i^{\text{combinatorial}} + \ln \gamma_i^{\text{residual}} + \ln \gamma_i^{\text{interfacial}} \quad (19.18)$$

$$\ln \gamma_i^{\text{interfacial}} = \frac{2\sigma v_i \sqrt[3]{(1-\phi_i)}}{RT r} \quad (19.19)$$

where

σ is the interfacial tension on micelle/water interface

v_i is the molar volume of the solute i

ϕ_i is the volume fraction of the solute i

r is the radius of the micelle

However, the modified UNIFAC-IF model still lacks a term of specific interactions between drugs and polymers.

The octanol–water partition coefficient ($\log P$) has been widely used to estimate the lipophilicity of a drug. It was first proposed by Hansch et al. to explain the relationship between the aqueous solubility of organic liquids and $\log P$,⁸⁹ which is expressed by

$$\log \left(\frac{1}{S} \right) = \log P + \frac{\mu_i^{\circ}(\text{oct}) - \mu_i^{\circ}(l)}{2.302RT} \quad (19.20)$$

where

S is the molar solubility of the organic liquid in water

P is its partition coefficient between 1-octanol and water

$\mu_i^{\circ}(\text{oct})$ is the chemical potential of the pure liquid solute in a 1 M ideal 1-octanol solution

$\mu(l)$ is the chemical potential of the pure liquid solute

The $\log P$ can be experimentally measured or calculated from structural features of a compound, using commercially available software.

Yalkowsky et al. expanded the application of octanol–water partition coefficient to the solubility of solid solutes. The activity coefficient of a solid solute ($\log \gamma^P$) is calculated from the equation

$$\log \gamma^P = \log P + 0.94 \quad (19.21)$$

In 1980, Yalkowski and Valvani proposed the general solubility equation (GSE) in which the crystallinity of a solute as well as the interaction of the solute with water are connected to the $\log P$ concept.⁹⁰ The GSE is

$$\log S_w = 0.5 - 0.01(\text{MP} - 25) \log K_{ow} \quad (19.22)$$

where

S_w is the molar aqueous solubility of a solute

MP is the melting point ($^{\circ}\text{C}$)

K_{ow} is the octanol–water partition coefficient ($=\log P$)

The GES reasonably predicted the solubility of numerous compounds.⁹¹ However, $\log P$ and $\log S_w$ still fail to explain the polymer–drug miscibility and the specific interactions between them.

Recently, the linear solvent free energy relationship (LSER) equation was employed to explain partition of solid solutes into micelles.^{92,93} The LSER assumes that drug partitioning between two immiscible phases is directly related to the transfer of free energy from water to the other phase (solvent or micelle). This free energy is the sum of independent and additive contributions of various drug–polymer interactions. Therefore, the LSER equation is expressed by

$$\log SP = c + rR_2 + s\pi_2 + a \sum \alpha_2 + b \sum \beta_2 + vV_x \quad (19.23)$$

where

SP is the property of interest for a solute or drug, i.e., partition coefficient

R_2 is the excess molar refraction of the solute (derived from the dispersion force)

π_2 is the solute dipolarity/polarizability

$\sum \alpha_2$ is the solute overall or effective hydrogen bond acidity

$\sum \beta_2$ is the solute overall or effective hydrogen bond basicity

V_x is the McGowan's characteristic volume calculated from molecular structure
($\text{cm}^3 \cdot \text{mol}^{-1}$)/100)

The c , r , s , a , b , and v refer to the regression coefficients obtained by compilation from database. Each individual component is determined either by multiple regression analysis based on measurement of partition coefficients (K in Equation 19.17)^{57,92–94} or by direct measurement.^{95–99} The LSER model contains various terms responsible for the drug–polymer interactions. In addition, the equation describes the miscibility of the polymer and the drug, which is applicable to polymer micelles. Therefore, LSER might be a good theory to explain the drug loading/solubilization mechanism of

hydrotropic polymer micelles or even of conventional micelles. Also, the equation can be used to design an efficient polymer micelle for a given drug.

19.4 STABILITY OF POLYMER MICELLE

The aqueous stability is another big issue to develop effective polymer micelles. Because a polymer micelle is a physically assembled structure in water, thermodynamic equilibrium and kinetic stability should be considered for practical application. Especially, the stability under biological condition is very important to accomplish successful delivery of therapeutic drugs. In this section, the stability of polymer micelles will be discussed from various angles.

19.4.1 STABILITY OF POLYMER MICELLE IN WATER AND BUFFERS

19.4.1.1 Thermodynamic Stability

Micelle is a structure in thermodynamic equilibrium, and in general, a closed association model is employed to explain micelle formation.¹⁰⁰ The strict closed association model is based on an all-or-none process, in which block copolymers (unimers) generate homogeneous micelles in size. As a result, an aqueous medium contains only unimers and monodisperse micelles. In pure water, the standard free energy change of micellization is

$$\Delta G^\circ = RT \ln(\text{CMC}) \quad (19.24)$$

where CMC is the critical micelle concentration.^{54,101,102} The CMC, that is the lowest polymer concentration to generate micelles by unimer aggregation, has significance in micelle stability. It may be reasonable, therefore, that micelles at equilibrium state will be destabilized (i.e., dissociated into unimers) when diluted. In general, higher MW of hydrophobic block provides the lower CMC value, which means more “stable.”¹⁰¹

Attwood et al. scored hydrophobicity of core-forming polymer blocks based on the analysis of CMC change as a function of the degree of polymerization (DP). For example, propylene oxide:lactic acid:ε-caprolactone is 1:4:12 triblock copolymer.¹⁰³ Logarithm curve of CMC vs. DP of a polyester (=block length) shows two transition points. As the DP increases, it is hypothesized that a long and linear chain of hydrophobic block spontaneously collapses, leading block copolymers to form unimeric or oligomeric micelles. Figure 19.7 shows a hypothetical mechanism to explain the relationship between log CMC and the DP of hydrophobic block. Line I (short dot, Figure 19.7A) shows Pluronic micelles, which are relatively hydrophilic block copolymers. Lines II and III shows block copolymers containing lactic acid and ε-caprolactone as repeating units of their hydrophobic blocks, respectively. When the DP of the hydrophobic block is ranged in B section, unimers are assembled to micelles above CMC (general closed association model, Figure 19.7B). Before the second transition point of DP, unimers and unimolecular micelles are equilibrated under a CMC, while they form a micelle over CMC (Figure 19.7C). A too high DP possibly makes all unimers to unimolecular micelles below CMC, which can be further aggregated as polymer concentration increases. Yamamoto et al. reported a similar description to explain a temperature-dependent change in CMC of PEG-*b*-PDLLA micelles.¹⁰⁴

These reports support the “bunchy micelle” model, in which the micellization occurs by aggregation of unimers with collapsed hydrophobic segments.¹⁰⁵ Since the stable geometry of the collapsed segments is a sphere, the micelle core may have many pores that are filled with solvents or drugs. However, it has been considered that the micelle core is a molten globule.⁵⁴ Usually, micelles are prepared from polymer solution of high concentration followed by removal of the solvent. Even though the preparation method is a thermodynamically quenching process, long polymer chains, especially hydrophobic polymer chains, are liable to be entangled together. If the time scale is

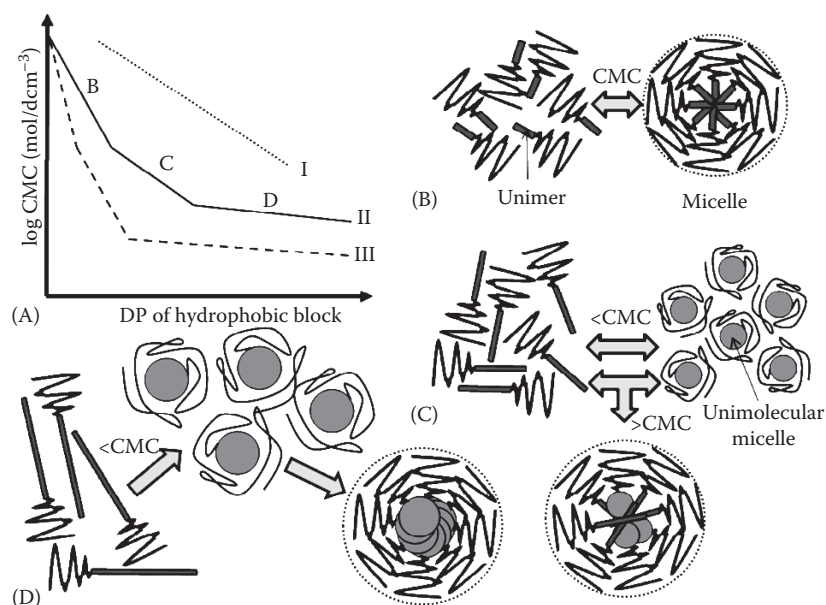


FIGURE 19.7 A hypothesis to explain unimolecular and multimolecular micelles. (A) Relationship between log CMC and the degree of polymerization (DP) of the hydrophobic block. The log CMC decreases as the hydrophobicity of the core-forming block increases (e.g., I: polypropylene, II: poly(D,L-lactide), and III: poly(ϵ -caprolactone)). (B) If the block length is short, there exists only unimer-micelle equilibrium. (C) As DP of the hydrophobic block increases, unimers collapse to unimolecular micelles. Over the CMC, multimolecular micelles are generated. (D) Hydrophobic block with high DP is spontaneously collapsed, and most of the unimers exist as unimolecular micelles. At higher polymer concentration, the unimolecular micelles aggregate further to form multimolecular micelles.

infinite, then all hydrophobic polymer chains can be converted to globular structures. As a result, micellization may be explained by combining the molten liquid core model and the bunchy micelle model together (Figure 19.8).

As described above, the CMC depends on the hydrophobicity of the core-forming block. However, it is also influenced by the crystallinity of hydrophobic blocks.^{106,107} For instance, the PDLLA, a kind of polyester, is an amorphous polymer, which has its glass transition temperature (T_g) around 55°C. Likewise, poly(lactide-co-glycolide) (PLGA) is an amorphous polymer (T_g ~50–60°C). However, poly(L-lactide) (PLLA) has high crystallinity with melting temperature (T_m) and T_g around 130°C and 60°C, respectively. Poly(ϵ -caprolactone) (PCL) is a semicrystalline polymer. T_m and T_g of PCL are ~55–65°C and –60°C, respectively.^{86,103,108} Isomers of D- and L-lactic acid in PDLLA influence the molecular configuration, which makes packing structure more spacey, i.e., more mobility of each PDLLA molecule. Glycolic acid, which loses a methyl group from lactic acid, is more hydrophilic, and also provides more space for the packing structure of PLGA.¹⁰⁹ Therefore, D-lactic acid and glycolic acid play the role of crystal structure breakers. Void volume at the micelle core is possessed by water molecules during micelle preparation. Therefore, micelle dissociation (relaxation) process can be more facilitated in short-term application to a diluted environment.

Block length ratio of diblock copolymers also controls CMC.^{101,103,110} The hydrophilic-lipophilic balance (HLB) is another expression of the block length ratio. For surfactant molecules containing PEG block, the HLB is equivalent to the mass percentage of oxyethylene content (E) divided by 5 ($HLB = E/5$).¹¹¹ Block copolymer with higher HLB value (more hydrophilic) generally decreases the CMC and increases the micelle size due to loose packing density.¹⁰¹ Diblock copolymer with $HLB < 10$ has a conical shape in water, which produces micellar structure by assembly. Polymers

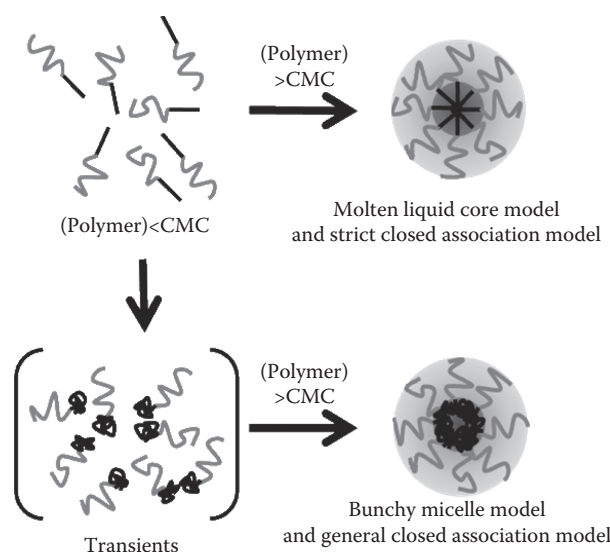


FIGURE 19.8 Two examples of micellization models. In relation to Figure 19.7, the molten liquid core model adopts a closed association model, in which only unimers and micelles are present in a system. In the bunchy micelle model, unimers are changed to unimolecular micelles by the collapsed hydrophobic block, which in turn produce multimolecular micelles.

with $HLB > 10$ can generate different shapes of supramolecular structure.^{112–114} If the hydrophobic block is long enough to be of cylinder shape in water, copolymer generates polymersome, which is very similar to the conformation of phospholipids.¹¹³

19.4.1.2 Kinetic Stability

Micelle association is a kinetic process, and similarly, micelle dissociation is the same. Aniansson and Wall (A–W) interpreted the dynamic mechanism of micelle relaxation.¹¹⁵ The A–W equations show that the exchange of unimers between micelles is a fast process and the decomposition of micelles into unimers is a slow process. The relationship between the number of unimers in a micelle and the concentration of micelles shows three continuous regions: the initial association (unimer-abundant) region, the intermediate region with unimer aggregates, and the micelle-abundant region. Because the aggregation process is very fast, micelle-containing solution will show a sharp bimodal distribution of the micelle size (either unimer- or micelle-dominant distribution). And, dissociation of unimers from micelles is governed by the internal free energy of micelles that is proportional to the length of hydrophobic blocks. However, experimental data have showed that this model (A–W model) of micelle relaxation was not always well-fit. This was because drastically simplified assumptions were made to explain the micelle relaxation process. The A–W model did not consider the micelle–micelle interaction, but only the fission mechanism was evaluated. A modified model, Gaussian model, suggests that the micelle relaxation depends on the fusion as well as the fission of micelles. By this model, the size distribution of micelles observed in experiments could be better explained.¹¹⁶

The A–W equations explain micelle relaxation by unimer dissociation and exchange between micelles, while the Gaussian model further suggests the size distribution of micelles by the fission–fusion mechanism. Studies on the exchange of unimers between micelles at equilibrium state supported the importance of fusion mechanism in micelle relaxation.^{117–119} To monitor the unimers exchange, nonradiative energy transfer (NET) was employed, which is known as the fluorescence (or Förster) resonance energy transfer (FRET). FRET is a physical process of transferring nonradiative energy from a donor fluorophore to an acceptor molecule.¹²⁰ This type of energy transfer is also

achievable between the same species of fluorophores (self-quenching). The transfer efficiency (E) is expressed as

$$E = k_T(\tau_D^{-1} + k_T) \quad (19.25)$$

where

k_T is the transfer rate

τ_D is the lifetime of donor in the absence of acceptors or self-quenching effect¹²⁰

For effective FRET, a donor molecule should be close enough to transfer its excitation energy to an acceptor (Figure 19.9). The transfer efficiency is inversely proportional to the sixth power of the distance (r) between donor and acceptor molecules:

$$E = \frac{R_0^6}{R_0^6 + r^6} \quad (19.26)$$

R_0 is known as the Förster distance at which a FRET pair of donor and acceptor shows 50% of transfer efficiency. The initial study was performed by Prochazka et al.¹²¹ They conjugated anthracene (FRET acceptor) or carbazole (FRET donor) to a block copolymer Kraton G-1701. By mixing micelles separately prepared from each dye-conjugated polymer, increase in fluorescence intensity from the anthracene was observed, while carbazole lowered its fluorescence emission.

Haliloglu et al. identified that the predominant mechanisms in the unimer exchange were insertion/expulsion and merger/splitting.¹¹⁹ The former mechanism is dominant at low polymer concentration and at high interaction energy between core-forming blocks (e.g., block length), while the latter mainly acts at high polymer concentration.

Insertion and expulsion of unimers during aggregation (oligomers or micelles) are governed by entropic free energy barrier. Therefore, either micellization or micelle decomposition is an activation process involving collective energy barriers, which can be explained by the internal free energy of micelle.^{100,122} The internal free energy of micelle suppresses association of too many unimers in a micelle (internal free energy of association, F_a) and dissociation of unimers from a micelle (internal free energy of dissociation, F_d). Due to F_a , a thermodynamic equilibrium of the micellization requires a very long time, which is not achievable in practical situations. As a result, micelles are loosely

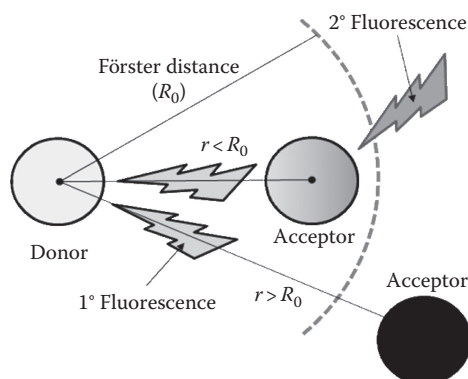


FIGURE 19.9 Fluorescence resonance energy transfer (FRET). If an acceptor dye exists within the Förster distance ($r < R_0$), fluorescence emission from a donor dye (1° fluorescence) will be used as excitation energy of the acceptor dye. As a result, fluorescence emission from acceptor (2° fluorescence) increases with decreased donor dye emission.

aggregated under experimental conditions. The F_d tends to prevent micelle disintegration. However, a “jump” condition, such as either dilution or increased temperature, provides enough energy for micelles to overcome the energy barrier, resulting in increased micelle disintegration.

The former mechanism is dominant at low polymer concentration and at high interaction energy between core-forming blocks (e.g., block length), while the latter mainly acts at high polymer concentration.

19.4.1.3 Drug Effect

Drugs loaded in polymer micelles can act as either plasticizers or fillers for the hydrophobic core. If the drug acts as a plasticizer, the friction of polymer chains will be reduced enough to decrease T_g of the hydrophobic core. In other words, addition of drug (plasticizer) will create more free volume in the micelle core. In contrast, filler effect will remove free volume from the polymer core.

The Kelley–Bueche equation expresses the effect of additives on effective T_g :

$$T_g = \frac{\phi_2 \alpha_2 T_{g2} + \phi_1 \alpha_1 T_{g1}}{\phi_2 \alpha_2 + \phi_1 \alpha_1} \quad (19.27)$$

where

ϕ is the volume fraction

α is the difference between volume extension factors above and below T_g

numerals 1 and 2, refer to the polymer and the drug, respectively¹²³

Although the above equation assumes diluted concentration of the additive, there exist some data showing that the drug acts as a plasticizer. For example, ketoprofen in PLGA polymer, microsphere in this case, decreased T_g of the polymer proportional to the drug loading amount.¹²⁴ On the contrary, there also exists some evidence that drug loading increases T_g . Quercetin effectively increased T_g of PCL block in PEG-*b*-PCL micelles, which proportionally depended on the drug loading amount.¹²⁵ Authors demonstrated that the increased T_g would be due to the hydrogen bonds between drug and carbonyl groups of PCL. Also, a poly(*N*-isopropylacrylamide-*co*-*N,N*-dimethylacrylamide)-*b*-PLGA (P(NIPAAm-*co*-DMAAm)-*b*-PLGA) micelle increased T_g of PLGA block by addition of paclitaxel.¹²⁶ As discussed previously, T_g of core-forming polymers should be important for micelle stability.

It has been believed that hydrophobic drugs may enhance the micelle stability primarily due to the hydrophobic effect, but there is not enough evidence to support this. It is more reasonable that the role of drugs is determined by the miscibility with hydrophobic polymer block. Actually, one unsolved problem of drug-loaded polymer micelles is the aqueous stability. Frequently, drug precipitation is observed when the micelles are stored in an aqueous medium, even though the micelle structure is not disrupted.^{82,83} It is explained by phase separation out of poor miscibility between the drug and the polymer.

19.4.2 STABILITY OF POLYMER MICELLE IN BIOLOGICAL ENVIRONMENTS

19.4.2.1 Micelle–Protein Interaction

Recently, Chen et al. clarified that a polymer micelle composed of PEG-*b*-PDLLA diblock copolymer was not stable in blood.¹²⁷ To investigate the stability of the micelle, a pair of FRET dyes (red and green) was loaded into the PEG-*b*-PDLLA micelles and injected into the bloodstream via tail vein. It was observed that the initial high FRET signal (0.886) significantly decreased in 15 min after injection down to 0.463. The FRET ratio was simply defined as

$$-\text{FRET} = \frac{I_R}{I_R + I_G} \quad (19.28)$$

where

I is the fluorescence intensity with arbitrary unit

R and G refer to the red and green dyes, respectively

In the experiments to examine the effect of blood components on the micelle stability, red blood cells did not show any significant interaction with the micelle. However, α - and β -globulins significantly destabilized the micelle, while albumin or γ -globulin was not responsible for decrease in the FRET ratio. Although they demonstrated the micelle stability in blood by an indirect method of loading FRET dyes, it was revealed that blood components, especially proteins, play a key role in micelle destabilization.

Polymer micelles have a similar property to amphiphilic surfactants in terms of micellization. Therefore, it is meaningful to predict the polymer micelle–protein interaction from surfactant–protein interaction. Interaction between surfactants and proteins has been extensively studied. In general, anionic surfactants exhibit relatively strong interaction leading to protein unfolding, while cationic surfactants weakly interact with proteins. For example, both cationic decyltriethylammonium bromide (DTAB) or anionic sodium decyl sulfonate (SDS) bind to bovine serum albumin (BSA), but a mixture of both surfactants, that made the net charge neutral, diminished interaction with BSA.¹²⁸ However, increase of hydrophobic parts in a cationic surfactant can significantly increase binding to proteins and their denaturation. For example, alkylenediyl- α,ω -bis(DTAB)s with hydrophobic alkyl chains showed BSA unfolding effect, which increased with alkyl chain length.¹²⁹

Nonionic surfactants have the weakest interactions with proteins, which is possibly explained by the lack of electrostatic interactions with proteins and their low CMC values.¹³⁰ It was reported that PEG-containing diblock copolymers also had interaction with BSA.¹³¹ The HLB of all copolymers used exceeded 10, so that at the CMC value the polymers formed 100–200 mM range micelles. As a result, interaction of block copolymers with BSA increased proportionally with the HLB value. This indicates that the major driving force of BSA–micelle (or block copolymer) interaction is the hydrophobic aggregation. Likewise, a micelle consisting of PEG-conjugated phospholipid (PEG₂₀₀₀-*b*-PE) is destabilized in the presence of BSA.¹³² At a high concentration of BSA (1%, w/v), the micelle structure was disrupted and BSA/PEG-*b*-PE aggregates were generated with increased particle size. A circular dichromism (CD) study showed that Trp in BSA structure was exposed to water at high concentration of BSA, but it was buried into a hydrophobic part of BSA as the BSA concentration increased. In a further study, it was found that the PEG-*b*-PE molecules were in contact with the Trp groups of BSA, leading to BSA unfolding and BSA/PEG-*b*-PE complexation.¹³³

19.4.2.2 PEG–Protein Interactions

PEG is a common and popular polymer used for micelle corona formation. PEG is nontoxic and biocompatible, but not totally inert under biological environments. The term biocompatibility is defined as the ability of a material to perform with an appropriate host response,¹³⁴ and does not necessarily mean the biological inertness. According to this definition, it can be considered that polymer micelles with the PEG shell are biocompatible rather than biologically inactive. However, polymer micelles have been described as stealth nanocarriers primarily due to the PEG outer shell. Because PEG has been used as a crystallizing agent for proteins instead of solvents or high concentration salts,^{135,136} it was considered that PEG has unfavorable

interaction with proteins leading to precipitation or crystallization.¹³⁷ Paradoxically, an aqueous two-phase partition system (ATPS) consisting of polymer and salt solution phases has been also used to extract proteins, in which proteins are dominantly located at the polymer (PEG) phase.¹³⁸ In addition, many evidences have shown that PEG does interact with biomolecules, especially proteins or lipids. As listed in Table 19.6, Rixman et al.

PEG interacts with biomolecules, especially proteins or lipids via the repulsive (primarily due to the chain flexibility and strong hydrogen bonding to water molecules) and attractive forces (hydrogen bonding, electrostatic, and van der Waals interactions). PEG has been reported to have direct interaction with proteins including lysozyme, fibronectin, serum albumin, pepsin, and α -chymotrypsin.

TABLE 19.6
Repulsive and Attractive Forces of PEG toward Serum Proteins

Repulsive	Attractive
Strong hydrogen bonding to water molecules	Hydrogen bonding
Entalpy restoration ^a	Electrostatic interaction ^c
Steric force due to the chain flexibility	van der Waals interaction (hydrophobic effect)
Hydrodynamic lubrication force ^b	

^a Incoming protein toward end-grafted PEG layer (e.g., micelle) may squeeze out water molecules from the layer, which is not entropically favorable.

^b Imposed motion of proteins toward PEG layer sets up a transverse pressure gradient.¹⁶

^c Oxygen atoms in PEG backbone have ability to chelate some cations such as Li⁺ or possibly Ca²⁺, which may electrostatically interact with charged proteins.^{17–19}

well summarized the repulsive (primarily due to the chain flexibility and strong hydrogen bonding to water molecules) and attractive forces (hydrogen bonding, electrostatic, and van der Waals interactions) of PEG to proteins in water.¹³⁹

Several reports elucidate that the PEG has direct interaction with proteins including lysozyme, fibronectin, serum albumin, pepsin,¹⁴⁰ and α -chymotrypsin.¹⁴¹ Furness et al. examined the interaction between PEG and hen-egg-white lysozyme by proton nuclear magnetic resonance (¹H-NMR) spectroscopy.¹⁴² By calculating maximal chemical shift change of amino acids upon PEG binding, it was found that six amino acids of the lysozyme Arg-61, Trp-62, Trp-63, Arg-73, Lys-96, and Asp-101 are selectively perturbed by PEG. The chemical shift change induced by PEG-poly(propylene oxide) block copolymer did not much differ from that observed by PEG treatment. However, a more hydrophilic polymer, poly(dihydroxypropyl methacrylate), significantly reduced change in the chemical shift. Based on these results, they concluded that the PEG-lysozyme binding was probably due to the hydrophobic interaction of the ethylene moieties of PEG.

Actually, PEG was a useful tool to detect soluble immune complexes from serum in systemic lupus erythematosus (SLE) and rheumatoid arthritis (RA).¹⁴³ Hurbert et al. found that fibronectin directly bound to the circulating immune complexes and in turn PEG could precipitate the immune complex.¹⁴⁴ Further, Robinson et al. demonstrated that many other non-immunoglobulin proteins such as fibronectin, haptoglobin, albumin, transferrin, and α -antitrypsin were also precipitated by 4% (w/v) PEG, and that the interaction between PEG and proteins was not nonspecific.¹⁴⁵

As described above, BSA binding to PEG-containing diblock copolymers was reduced proportional to the PEG length (or polymer HLB).¹³¹ However, it was disproved that the BSA could bind to the micelles to some extent. There are some evidences to show that serum albumin directly binds to PEG. Cocke et al. examined the interaction between PEG and human serum albumin (HSA) by affinity capillary electrophoresis (ACE).¹⁴⁶ Upon PEG binding with HAS, the enthalpy change was 19.1 kJ/mol and the entropy change was 16.6 J/mol·K, which led to the total free energy change of -31.4 kJ/mol. The negative but small change of the free energy implies that binding of HSA to PEG is a thermodynamically favorable (or spontaneous) reaction, and that the HSA-PEG interaction is forced primarily by entropy change.

Similar phenomenon was observed from isothermal titration calorimetry (ITC) of lysozyme and ovalbumin.¹⁴⁷ Rixman et al. directly measured the force between PEG and HSA using HSA-coated molecular force probe.¹³⁹ The binding force of HSA-coated probe to individual PEG chain was determined as 0.06 ± 0.1 nN, which was primarily attributed to hydrogen bonding and van der Waals interaction (or hydrophobic effect) between PEGs and HSAs. Hydrogen bond between PEG and HSA was also confirmed by Fourier transform-infrared (FT-IR) spectroscopy.¹⁴⁸ CD spectra revealed that PEG forming a complex with HSA denatured the secondary structure of the albumin.

Based on a database for protein crystal structures in the presence of PEG, Hasek found four modes of the interaction between PEG and proteins: (1) multiple coordination via positively charged amino acids, i.e., Lys, Arg, His; (2) hydrogen bonding of amino acid side groups; (3) hydrogen bonding of backbone amide group; and (4) cation coordination.¹⁴⁹

In summary, it is highly possible that polymer micelles composed of PEG-containing block copolymers are not completely inert in a body. Interactions between serum proteins and PEG corona of micelles have been frequently observed. The PEG shell of a micelle is known to expel serum proteins by hydrated chain mobility. However, the protein penetration into micelle has been also observed as described in the following section.

19.4.2.3 Protein Penetration into Micelles

Exposure of hydrophobic segments of micelles should eventually induce protein adsorption and denaturation because poor biocompatibility of a certain material mostly originates from its hydrophobicity.¹⁵⁰ In polymer micelles, the hydrophilic PEG shell has been considered as a shield preventing the hydrophobic micelle core from direct contact to biological constituents. As described above, however, the PEG molecule apparently has activities in blood that may provoke micelle destabilization. In contrast, there is another possibility that unimers from destabilized micelles interact with proteins or lipid membranes, even though no evidence has been found.

Protein penetration into micelles can also reduce micelle stability in blood. Li et al. observed that lipase slowly degraded the PCL block of PEG-*b*-PCL micelles, although the degradation rate was slower than the PCL-*b*-PEG-*b*-PCL triblock copolymer or the PCL homopolymer.¹⁵¹ The mechanism of action of lipase K is to hydrolyze fatty acids, but it is also able to cleave the polyester backbone such as PCL. Adsorption of lipase onto PCL surface was the necessary condition for enzymatic activity.¹⁵² Hydrolysis of the ester backbone catalyzed by lipase is limited to the amorphous region of PCL polymer matrix because PCL is a semicrystalline polymer, as mentioned previously.^{152,153}

Carstens et al. investigated the kinetics of enzymatic hydrolysis of a micelle consisting of PEG₇₅₀ and oligo-PCL (degree of polymerization, DP, ~5).¹⁵⁴ According to the Michaelis–Menten equation, the Michaelis constant, V_m , representing the maximal rate of enzymatic activity was $4.4 \pm 0.2 \mu\text{mol}/\text{min}$, and K_m of the maximal binding affinity of lipase to PCL was $2.2 \pm 0.3 \text{ mg}/\text{mL}$ at an enzyme concentration of $19 \text{ mU}/\text{mL}$. Also, they proposed that there were two possibilities of lipase-catalyzed PCL degradation, viz., hydrolysis of unimers dissociated from micelles and degradation of micelle core via lipase penetration. In experiments examining biodegradation of a polymer micelle composed of a triblock copolymer, PEG-*b*-poly(3-hydroxybutyrate)-*b*-PEG (PEG-*b*-PHB-*b*-PEG), hydrolysis of the PHB polymer block by extracellular PHB depolymerase depended on the enzyme concentration, initial polymer concentration, and PHB block length.¹⁵⁵ Authors demonstrated that the amorphous core of micelles was enzyme penetrable. Hence, it is highly probable that protein penetration induces micelle instability under a biological condition.

19.4.3 MICELLE–CELL INTERACTION

Two possible interactions exist between polymer micelles and cells, viz., cellular uptake and cell membrane perturbation, although mechanisms of these events are not clear yet. As described in the previous section, PEGs or micelles can interact with proteins, which is a possible mechanism. Cellular internalization, or endocytosis, can be accomplished by either phagocytosis or pinocytosis.^{156,157} Relatively large particles are engulfed by phagocytosis, which is mediated by pseudopods extended from cell surface. Pinocytosis is frequently mediated by clathrin^{158,159} and caveolae.¹⁶⁰ Both these pathways include dynamin polymerization for vesicle budding. There exist many nonspecific pathways of endocytosis, including a clathrin- and dynamin-independent pathway.¹⁵⁶ Recently, Stephanie et al. demonstrated that polymer particles with high homogeneity in size are endocytosed either by phagocytosis and clathrin-mediated endocytosis.¹⁶¹ The endocytosis depended on the particle size: particles with submicron size showed faster uptake than few micron-sized particles.

If the hydrophilic shell is a stealth coat of polymer micelles, their internalization will be much inhibited. Recently, Chen et al. showed that a polymer micelle composed of PEG-*b*-PDLA and fluorescein isothiocyanate (FTIC)-PEG-*b*-PDLA did not enter into cultured HeLa cells.¹⁶² When the cancer cells were incubated with polymer micelles of PEG-*b*-PDLA loading a FRET dye pair, the hydrophobic dyes were observed in the cytoplasmic compartment. These results demonstrate the diffusion of hydrophobic molecules (e.g., drugs) across the cell membrane, rather than the internalization of whole micelle.

Nevertheless, evidence of micelle internalization has been reported. A polymer micelle of Pluronic P85 effectively accumulated a hydrophobic fluorescent probe inside living cells. At lower concentration, effect of the P85 on cellular accumulation of the dye was mediated by preventing the pump-out mechanism of P-glycoprotein (P-gp), but at higher concentration, vesicular transport was facilitated by the Pluronic.¹⁶³ In another experiment, pH-sensitive dye-labeled Pluronic (P105) was also observed inside various cancer cells, including multidrug resistance (MDR) cell lines.¹⁶⁴ P105 internalization increased the membrane permeability resulting in effective drug uptake by MDR cells. Later, Sahay et al. revealed that internalization of the P85 had two different pathways: caveolae-mediated endocytosis at lower concentration (<CMC) and clathrin-mediated endocytosis at higher concentration (>CMC).¹⁵⁷ The authors suggested a possibility that the interaction of the hydrophobic polymer block with caveolin may cause P-gp inhibition as well as other intracellular events, including gene expression. It was revealed that the most effective structure of Pluronic has HLB < 20.¹⁶⁵ Similarly, P-gp inhibition was also induced by the PEG-*b*-PCL block copolymer at a concentration below the CMC.¹⁶⁶ It is highly probable that the PEG-*b*-PCL has the same mechanism, viz., unimer-mediated lipid raft (e.g., caveolae) interruption, as pluronics inhibit P-gp.

It has been often reported that polymer micelles consisting of PEG-*b*-PCL at high concentration (>CMC) can be internalized. Allen et al. showed that a PEG-*b*-PCL micelle loading a fluorescent probe was effectively localized inside PC12 cells.¹⁶⁷ Also, the cellular uptake of ³H-labeled FK506 was much improved by the micelle carrier comparing to free FK506. However, internalization of either fluorescent dye or isotope-labeled drug may not exactly reflect the micelle endocytosis. Later, they visualized internalization of blank polymer micelle using rhodamine-labeled PEG-*b*-PCL (PEG-*b*-PCL-Rh)¹⁶⁸ and endocytosis of a drug-containing polymer micelle.¹⁶⁹ Moghimi et al. suggested a refutation that stressed the role of fluorescent dye.¹⁷⁰ Because rhodamine is positively charged, electrostatic attraction is possibly responsible for cellular uptake of the micelle. Also, PEG-*b*-PCL micelle endocytosis might depend on characteristics of used cells¹⁷¹ and the MW of the hydrophobic or the hydrophilic block.¹⁷²

The micelle endocytosis observed in cultured cells cannot provide enough evidence to clarify whether the internalization process really happens *in vivo*. *In vitro* experiments are usually performed in a static culture of cancer cell lines incubated with a high concentration of polymer micelles. Limitations of the *in vitro* culture systems arise from the deficiency of whole blood components and various cell types, the monolayer of cultured cells exposing maximum surface area to the environment, the lack of biochemical dynamics present in a living organism, and the localization of high concentration of polymers.

On the other hand, membrane perturbation by unimers dissociated from micelles is another possible interaction mechanism between micelles and cells. As discussed above, Pluronic and PEG-*b*-PCL block copolymers showed an interesting activity on P-gp inhibition at concentrations below their CMCs. Discher and Ahmed suggested that hemolytic activity of block copolymers are highly related to their HLB and MW.¹¹³ A high value of HLB may generate a cylinder-like unimer structure, similar to the shape of phospholipids, which possibly facilitates membrane disruption. Additional activity of Pluronic (poloxamer 188; P188) on cells is the membrane-sealing effect. It was first demonstrated in electroporabilized skeletal muscle cells,¹⁷³ which was recently confirmed by the magnetic resonance imaging (MRI) technique.¹⁷⁴ Numerous reports indicate that P188 is very effective in healing damaged plasma membrane *in vitro* and *in vivo*.¹⁷⁵ P188 binds to the lipid bilayer where the packing density is locally low. It is also possible that the PEG shell of polymer micelles

mediates the membrane sealing. It is well known that the PEG provokes lipid membrane fusion and a critical PEG concentration is required for membrane fusion.¹⁷⁶ Due to the water-trapping ability of PEG, free water content around cells might be reduced. This is believed as one mechanism inducing lipid molecule exchange between phospholipid vesicles.^{177,178}

Membrane curvature, which alters outer leaflet packing density, and the small impurities in membrane vesicles (e.g., unsaturated acryl chain of phospholipids) effectively lower the threshold concentration of PEG for membrane fusion.^{179,180} For this reason, PEG is a potential therapeutic material to restore the damaged membrane. For example, PEG has excellent healing effect on injured spinal cords via the membrane-sealing mechanism.^{181,182} If PEG induces local dehydration around cell membrane and block copolymers nonspecifically bind to lipid rafts, as mentioned above, then the insertion of unimers dissociated from micelles, the disruption of plasma membrane, or cell-cell fusion are highly possible.

19.4.4 *IN VIVO* STABILITY OF POLYMER MICELLES

Polymer micelles as drug carriers should be stable in the bloodstream to deliver drugs to target sites or to improve the pharmacokinetics of the drug. However, prediction about *in vivo* stability of polymer micelles is very difficult because of the biological and the physiological complexity of a living organism. In addition to the thermodynamic and kinetic stability issues in an aqueous medium and the interaction of polymer micelles with biomolecules, continuous flow of blood, the presence of many kinds of cell types, organ-specific physiological function, and diversity of individuals produce a totally complicated biological barrier. Although *in vitro* characterization methods for micelle stability may provide an insight to design carrier systems and appropriate *in vivo* experimental setups, there is no practical method to evaluate micelle stability *in vivo*.

The fate of micelles after intravenous administration has been frequently monitored by labeling with radioisotopes, as summarized in Table 19.7. Valuable information was obtained about the *in vivo* fate of polymer micelles. In the study using ³H-labeled Pluronic P85, higher concentration of polymers, especially over the CMC, showed much longer circulation time.¹⁸³ It indicated that the polymer micelle is not immediately dissociated in bloodstream. The primary location of polymers was in blood. However, polymer micelles are likely to end up in liver and spleen, where the RES system is working. In other words, the stealth hydrophilic shell of micelles might not be good enough to escape the host defense system. However, radioisotope labeling studies lack direct evidence for *in vivo* micelle stability, because unimers dissociated from micelles and even their degraded products show radioactivity.

19.5 PERSPECTIVES AND CONCLUSIVE REMARKS

Polymer micelles present a great potential to formulate and deliver poorly soluble drugs. However, their two major limitations, low drug loading capacity and aqueous instability, remain unresolved. Hydrotropy is a potential solution alleviating the problems associated with drug loading. To obtain an efficient polymeric micelle carrier, extensive research on polymer-drug compatibility should be carried out. Based on understanding about interactions between polymers and drugs, strategies can be developed to improve micelle stability.

Optical imaging techniques, including FRET, opened a new possibility to examine the *in vitro* and *in vivo* stability of micelles. The radio-labeling method to determine the biodistribution of polymer micelles could not fully reflect the micelle stability *in vivo*. Also, it is an invasive method inducing damage to cells and tissues. Tissue damage may alter physiological response to polymer micelles. Recent advances in molecular imaging techniques allow noninvasive imaging at molecular and sub-cellular levels. In particular, fluorescence imaging techniques can provide useful tools to observe micelle stability due to easy accessibility at a lab scale and moderate cost of imaging instruments.¹⁸⁴ In addition to *in vivo* stability monitoring, micelles loaded with imaging agents can be applied as

TABLE 19.7
Studies on Biodistribution of Polymer Micelles

Polymer	Building Blocks		Drug	Micelle Size (nm)	Label	Biodistribution	Reference
	Block Length (kDa)	Drug					
PEG _x - <i>b</i> -PCL _y	$x = 6.0, y = 1.0$	N/A	N/A	60	¹²⁵ I-PEG	In 1 and 24 h after tail vein injection, blood > bone > kidney > liver > lung > brain	[20]
	$x = 5.0, y = 5.0$	N/A	N/A	56	³ H-PCL	Liver > kidney > spleen, lung > heart; biodistribution profile did not change much up to 48 h after tail vein injection regardless of initial dose	[21]
PEG _x - <i>b</i> -PLA _y	$x = 2.0, y = 2.4$	N/A	N/A	~25	F-5-CADA (fluorescent)	In 1 h after intramuscular or subcutaneous injection, micelle disintegration was observed; Too bright background fluorescence from mice	[22]
	$x = 5.0, y = 7.0$	N/A	N/A	300	¹²⁵ I-PLA	Micelle with smaller size was cleared faster in spite of longer PEG. In 2 h after tail vein injection, blood > bowel (inflamed site) > liver > kidney > spleen	[23]
	$x = 14.0, y = 6.0$ $x = 5.0, y = 5.0$	N/A N/A	N/A N/A	72 300	¹²⁵ I-PLA	Blood > liver > kidney > lung, heart, spleen; With time, radioactivity gradually decreased without changing the organ distribution	[24]
PEG _i - <i>b</i> -PA _{sp} -Dox	$x = 5.1, y = 5.3$	N/A	N/A	37–38	¹²⁵ I-Tyr; ¹²⁵ I-Tyr-Glu	Liver > kidney > lung, spleen; With time, liver and spleen showed more radioactivity while kidney and lung decreased it; No significant effect of anionic amino acid (Glu)	[25]
	$x = 2.0, y = 2.0$	Ptx	Ptx	—	¹⁴ C-PDLLA or ¹⁴ C-PEG	Plasma elimination half life was 2.6–2.9 h	[26]
	$x = 4.3, y = 1.9$	Dox	Dox	~50	¹²⁵ I-PEG	In 1 h after tail vein injection, blood (17.1% ± 2.3% dose/g) > spleen > kidney > liver > lung > heart	[27]

(continued)

TABLE 19.7 (continued)
Studies on Biodistribution of Polymer Micelles

Polymer	Building Blocks		Micelle Size (nm)	Label	Biodistribution	Reference
	Block Length (kDa)	Drug				
PAA _x - <i>b</i> -PMAA _y	<i>x</i> = 4.8, <i>y</i> = 18.6	N/A	~24	⁶⁴ Cu (PET)	Shell crosslinked by a bifunctional amine and coated with PEG _{5,400} ; Spleen > liver > kidney > blood > lung regardless of polymer block length; No PEG effect	[28]
	<i>x</i> = 6.0, <i>y</i> = 7.0	N/A	~37			
PAA _x - <i>b</i> -PS _y	<i>x</i> = 6.0, <i>y</i> = 7.0	N/A	19–22	⁶⁴ Cu (PET)	Shell crosslinked by a bifunctional amine and coated with PEG _{2,000} ; Micelles with lower PEG density showed spleen > liver > kidney > lung > blood; micelles with higher PEG density showed spleen > liver, blood > lung > kidney	[29]
	<i>x</i> = 8.7, <i>y</i> = 7.4	N/A	~18	⁶⁴ Cu (PET)	Shell crosslinked by a bifunctional amine and coated with PEG _{5,400} ; random distribution	[28]
PEO _x - <i>b</i> -PPO _y - <i>b</i> -PEO _z (P85)	<i>x</i> = 6.0, <i>y</i> = 15.4	N/A	~37			
	<i>x</i> = 1.2, <i>y</i> = 2.3	N/A	1.5 [31]	³ H	The higher dose led to the larger AUC; Only over the CMC, the circulation time was prolonged; Liver > spleen > kidney > lung > brain	[30]

Note: AUC, area under curve; Dox, doxorubicin; F-5-CADA, fluorescein-5-carboxyl azide diacetate; Glu, glutamic acid; N/A, not applied; PAA, poly(acrylic acid); PAsp, poly(aspartic acid); PCL, poly(ϵ -caprolactone); PE, phosphatidylethanolamine; PEG, poly(ethylene glycol); PEO, poly(ethylene oxide); PET, Positron emission tomography, PLA, poly(D,L-lactide); PMAA, poly(methacrylate); PPO, poly(propylene oxide); PS, poly(styrene); PtX, paclitaxel; Tyr, tyrosine.

molecular imaging probes. Multifunctional micelles performing drug delivery and molecular imaging allow simultaneous therapy and imaging by the same system.^{42,185}

The poor stability of micelles in water and biological media originates from the physical association of unimers. Chemical crosslinking between unimers can improve micelle stability. The CMC is no more valid in crosslinked micelles, so that aqueous instability upon dilution is obviated as an issue. Various versions of crosslinked micelles have been developed.^{186,187} In Table 19.7, PAA-*b*-PMAAs and PAA-*b*-PS are examples for shell-crosslinked micelles. In those micelles, an additional layer of PEG was coated to improve the biocompatibility.^{188,189} A macromonomer of PEG-*b*-PCL with a polymerizable vinyl group at the PCL end led to a core-crosslinked micelle mediated by a radical initiator.¹⁹⁰ The crosslinked PEG-*b*-PCL micelle showed fair efficiency in paclitaxel loading property. Although such crosslinked micelles are expected to improve aqueous stability, additional modification steps with highly reactive chemicals as well as no or slow degradation of block copolymers may be unfavorable for a drug delivery system. An interesting example of crosslinked micelles is the interfacial crosslinking with reversible disulfide bridges.¹⁹¹ Disulfide bonds can be reduced by glutathione that exists in cells. Application of crosslinked micelles in the drug delivery field is still limited, but due to the advantage of structural integrity, they have a great potential to improve the micellar drug delivery system.

Since the assembly/disassembly of micelles highly depends on the structure of block copolymer, it is also important to design and prepare polymers with well-controlled structure. The combinatorial synthetic strategy in polymerization (parallel synthesis) now provides a great chance to prepare numerous polymers in a simple manner.^{192,193} In addition to the high-throughput synthetic method, controlled radical polymerization (CRP) methods, including atom transfer radical polymerization (ATRP), reversible addition fragmentation chain transfer (RAFT) polymerization, and nitroxide-mediated polymerization (NMP), are useful in synthesizing well-defined block copolymers.^{194–196} The CRP methods provide not only controllability of polymer structure/topology, but also functionality of block copolymers to conjugate ligands or imaging agents. Micelle stability under physiological conditions can also be improved by polymer chemistry.

The disintegration of polymer micelles depending on a certain stimulus is now an important strategy in the micellar drug delivery system. Smart materials actively change their physicochemical properties responding to the environmental signals. Such smart polymers have been aggressively employed to improve therapeutic efficacy and to reduce undesirable side effects of drugs.¹⁹⁷

In conclusion, two limitations of polymer micelles in drug delivery, the low drug loading capacity and aqueous instability, need to be overcome. These limitations also provide a new opportunity to improve the micellar drug delivery system, via advanced technologies in polymer chemistry and molecular imaging. Polymer micelles are currently undergoing evolution to become a useful tool for clinical applications. Increasing research interest is expected in the mechanisms on micellar interaction with drug, biomolecules, or cells.

REFERENCES

1. Lombardino JG, Lowe JA, 3rd, The role of the medicinal chemist in drug discovery—Then and now. *Nat Rev Drug Discov* 2004; **3**: 853–862.
2. Kramer JA, Sagartz JE, Morris DL, The application of discovery toxicology and pathology towards the design of safer pharmaceutical lead candidates. *Nat Rev Drug Discov* 2007; **6**: 636–649.
3. Lipinski CA, Drug-like properties and the causes of poor solubility and poor permeability. *J Pharmacol Toxicol Methods* 2000; **44**: 235–249.
4. Maeda H, Wu J, Sawa T, Matsumura Y, Hori K, Tumor vascular permeability and the EPR effect in macromolecular therapeutics: A review. *J Control Release* 2000; **65**: 271–284.
5. Maeda H, Sawa T, Konno T, Mechanism of tumor-targeted delivery of macromolecular drugs, including the EPR effect in solid tumor and clinical overview of the prototype polymeric drug SMANCS. *J Control Release* 2001; **74**: 47–61.

6. Iyer AK, Greish K, Seki T, Okazaki S, Fang J, Takeshita K, Maeda H, Polymeric micelles of zinc protoporphyrin for tumor targeted delivery based on EPR effect and singlet oxygen generation. *J Drug Target* 2007; **15**: 496–506.
7. Paciotti GF, Myer L, Weinreich D, Goia D, Pavel N, McLaughlin RE, Tamarkin L, Colloidal gold: A novel nanoparticle vector for tumor directed drug delivery. *Drug Deliv* 2004; **11**: 169–183.
8. Dobrovolskaia MA, Aggarwal P, Hall JB, McNeil SE, Preclinical studies to understand nanoparticle interaction with the immune system and its potential effects on nanoparticle biodistribution. *Mol Pharm* 2008; **5**: 487–495.
9. Kim TY, Kim DW, Chung JY, Shin SG, Kim SC, Heo DS, Kim NK, Bang YJ, Phase I and pharmacokinetic study of Genexol-PM, a cremophor-free, polymeric micelle-formulated paclitaxel, in patients with advanced malignancies. *Clin Cancer Res* 2004; **10**: 3708–3716.
10. Kim DW, Kim SY, Kim HK, Kim SW, Shin SW, Kim JS, Park K, Lee MY, Heo DS, Multicenter phase II trial of Genexol-PM, a novel Cremophor-free, polymeric micelle formulation of paclitaxel, with cisplatin in patients with advanced non-small-cell lung cancer. *Ann Oncol* 2007; **18**: 2009–2014.
11. Lee KS, Chung HC, Im SA, Park YH, Kim CS, Kim SB, Rha SY, Lee MY, Ro J, Multicenter phase II trial of Genexol-PM, a Cremophor-free, polymeric micelle formulation of paclitaxel, in patients with metastatic breast cancer. *Breast Cancer Res Treat* 2008; **108**: 241–250.
12. Matsumura Y, Hamaguchi T, Ura T, Muro K, Yamada Y, Shimada Y, Shirao K et al., Phase I clinical trial and pharmacokinetic evaluation of NK911, a micelle-encapsulated doxorubicin. *Br J Cancer* 2004; **91**: 1775–1781.
13. Negishi T, Koizumi F, Uchino H, Kuroda J, Kawaguchi T, Naito S, Matsumura Y, NK105, a paclitaxel-incorporating micellar nanoparticle, is a more potent radiosensitising agent compared to free paclitaxel. *Br J Cancer* 2006; **95**: 601–606.
14. Danson S, Ferry D, Alakhov V, Margison J, Kerr D, Jowle D, Brampton M, Halbert G, Ranson M, Phase I dose escalation and pharmacokinetic study of pluronic polymer-bound doxorubicin (SP1049C) in patients with advanced cancer. *Br J Cancer* 2004; **90**: 2085–2091.
15. Merisko-Liversidge EM, Liversidge GG, Drug nanoparticles: Formulating poorly water-soluble compounds. *Toxicol Pathol* 2008; **36**: 43–48.
16. Serajuddin AT, Salt formation to improve drug solubility. *Adv Drug Deliv Rev* 2007; **59**: 603–616.
17. Attwood D, Thermodynamic properties of amphiphilic drugs in aqueous solution. *J Chem Soc Faraday Trans I* 1989; **85**: 3011–3017.
18. Kesisoglou F, Panmai S, Wu Y, Nanosizing—oral formulation development and biopharmaceutical evaluation. *Adv Drug Deliv Rev* 2007; **59**: 631–644.
19. Rabinow BE, Nanosuspensions in drug delivery. *Nat Rev Drug Discov* 2004; **3**: 785–796.
20. Keck CM, Muller RH, Drug nanocrystals of poorly soluble drugs produced by high pressure homogenisation. *Eur J Pharm Biopharm* 2006; **62**: 3–16.
21. Strickley RG, Solubilizing excipients in oral and injectable formulations. *Pharm Res* 2004; **21**: 201–230.
22. Buggins TR, Dickinson PA, Taylor G, The effects of pharmaceutical excipients on drug disposition. *Adv Drug Deliv Rev* 2007; **59**: 1482–1503.
23. Brewster ME, Loftsson T, Cyclodextrins as pharmaceutical solubilizers. *Adv Drug Deliv Rev* 2007; **59**: 645–666.
24. Loftsson T, Duchene D, Cyclodextrins and their pharmaceutical applications. *Int J Pharm* 2007; **329**: 1–11.
25. Osterberg RE, See NA, Toxicity of excipients—a Food and Drug Administration perspective. *Int J Toxicol* 2003; **22**: 377–380.
26. Dye D, Watkins J, Suspected anaphylactic reaction to Cremophor EL. *Br Med J* 1980; **280**: 1353.
27. Strachan EB, Case report—suspected anaphylactic reaction to Cremophor EL. *SAAD Dig* 1981; **4**: 209.
28. Barrow PC, Olivier P, Marzin D, The reproductive and developmental toxicity profile of beta-cyclodextrin in rodents. *Reprod Toxicol* 1995; **9**: 389–398.
29. Lina BA, Bar A, Subchronic (13-week) oral toxicity study of alpha-cyclodextrin in dogs. *Regul Toxicol Pharmacol* 2004; **39**(Suppl 1): S27–S33.
30. Ulloth JE, Almaguel FG, Padilla A, Bu L, Liu JW, De Leon M, Characterization of methyl-beta-cyclodextrin toxicity in NGF-differentiated PC12 cell death. *Neurotoxicology* 2007; **28**: 613–621.
31. Serajuddin AT, Solid dispersion of poorly water-soluble drugs: Early promises, subsequent problems, and recent breakthroughs. *J Pharm Sci* 1999; **88**: 1058–1066.
32. Chawla G, Bansal AK, Improved dissolution of a poorly water soluble drug in solid dispersions with polymeric and non-polymeric hydrophilic additives. *Acta Pharm* 2008; **58**: 257–274.

33. Chiou WL, Riegelman S, Preparation and dissolution characteristics of several fast-release solid dispersions of griseofulvin. *J Pharm Sci* 1969; **58**: 1505–1510.
34. Van Balen GP, Martinet GM, Caron G, Bouchard G, Reist M, Carrupt PA, Fruttero R, Gasco A, Testa B, Liposome/water lipophilicity: Methods, information content, and pharmaceutical applications. *Med Res Rev* 2004; **24**: 299–324.
35. Bangham AD, Horne RW, Negative staining of phospholipids and their structural modification by surface-active agents as observed in the electron microscope. *J Mol Biol* 1964; **8**: 660–668.
36. Torchilin VP, Recent advances with liposomes as pharmaceutical carriers. *Nat Rev Drug Discov* 2005; **4**: 145–160.
37. Gabizon AA, Shmeeda H, Zalipsky S, Pros and cons of the liposome platform in cancer drug targeting. *J Liposome Res* 2006; **16**: 175–183.
38. Liu D, Liu F, Song YK, Recognition and clearance of liposomes containing phosphatidylserine are mediated by serum opsonin. *Biochim Biophys Acta* 1995; **1235**: 140–146.
39. Yan X, Scherphof GL, Kamps JA, Liposome opsonization. *J Liposome Res* 2005; **15**: 109–139.
40. Papisov MI, Theoretical considerations of RES-avoiding liposomes: Molecular mechanics and chemistry of liposome interactions. *Adv Drug Deliv Rev* 1998; **32**: 119–138.
41. Chiu GN, Bally MB, Mayer LD, Selective protein interactions with phosphatidylserine containing liposomes alter the steric stabilization properties of poly(ethylene glycol). *Biochim Biophys Acta* 2001; **1510**: 56–69.
42. Torchilin V, Multifunctional and stimuli-sensitive pharmaceutical nanocarriers. *Eur J Pharm Biopharm* 2009; **71**: 431–444.
43. Amsberry KL, Borchardt RT, Amine prodrugs which utilize hydroxy amide lactonization. I. A potential redox-sensitive amide prodrug. *Pharm Res* 1991; **8**: 323–330.
44. Cook CS, Karabatsos PJ, Schoenhard GL, Karim A, Species dependent esterase activities for hydrolysis of an anti-HIV prodrug glycovir and bioavailability of active SC-48334. *Pharm Res* 1995; **12**: 1158–1164.
45. Riley CM, Mummert MA, Zhou J, Schowen RL, Vander Velde DG, Morton MD, Slavik M, Hydrolysis of the prodrug, 2',3',5'-triacetyl-6-azauridine. *Pharm Res* 1995; **12**: 1361–1370.
46. Springer CJ, Niculescu-Duvaz II, Antibody-directed enzyme prodrug therapy (ADEPT): A review. *Adv Drug Deliv Rev* 1997; **26**: 151–172.
47. Chen L, Waxman DJ, Cytochrome P450 gene-directed enzyme prodrug therapy (GDEPT) for cancer. *Curr Pharm Des* 2002; **8**: 1405–1416.
48. Ringsdorf H, Structure and properties of pharmacologically active polymers. *J Polym Sci Polym Symp* 1975; **51**: 135–153.
49. Li C, Wallace S, Polymer-drug conjugates: Recent development in clinical oncology. *Adv Drug Deliv Rev* 2008; **60**: 886–898.
50. Kratz F, Muller IA, Ryppa C, Warnecke A, Prodrug strategies in anticancer chemotherapy. *Chem Med Chem* 2008; **3**: 20–53.
51. Hildebrand JH, A critique of the theory of solubility of non-electrolytes. *Chem Rev* 1949; **44**: 37–45.
52. Zeng W, Du Y, Xue Y, Frish HL, in *Physical Properties of Polymer Handbook*. E. M. James (Ed.) (Springer-Verlag New York, LLC, New York, 2006).
53. Flory PJ, *Principle of Polymer Chemistry* (Cornell University Press, Ithaca, NY, 1953).
54. Liu R, Forrest ML, Kwon GS, in *Water-Insoluble Drug Formulation*. R. Liu (Ed.) (CRS Press, Taylor & Francis Group, New York, 2008).
55. Adamska K, Voelkel A, Inverse gas chromatographic determination of solubility parameters of excipients. *Int J Pharm* 2005; **304**: 11–17.
56. Liu J, Xiao Y, Allen C, Polymer–drug compatibility: A guide to the development of delivery systems for the anticancer agent, ellipticine. *J Pharm Sci* 2004; **93**: 132–143.
57. Letchford K, Liggins R, Burt H, Solubilization of hydrophobic drugs by methoxy poly(ethylene glycol)-block-polycaprolactone diblock copolymer micelles: Theoretical and experimental data and correlations. *J Pharm Sci* 2008; **97**: 1179–1190.
58. Burt HM, Zhang XC, Toleikis P, Embree L, Hunter WL, Development of copolymers of poly(D,L-lactide) and methoxypolyethylene glycol as micellar carriers of paclitaxel. *Colloids Surf B Biointerfaces* 1999; **16**: 161–171.
59. Vippagunta SR, Brittain HG, Grant DJ, Crystalline solids. *Adv Drug Deliv Rev* 2001; **48**: 3–26.
60. Coffman RE, Kildsig DO, Hydrotropic solubilization—Mechanistic studies. *Pharm Res* 1996; **13**: 1460–1463.
61. Matero A, in *Handbook of Applied Surface and Colloid Chemistry*. K. Holmberg (Ed.) (John Wiley & Sons, New York, 2001).

62. Ooya T, Lee S, Huh KM, Park K, in *Nanocarrier Technologies: Frontiers of Nanotherapy*. M. R. Mozafari (Ed.) (Springer, Amsterdam, the Netherlands, 2006).
63. Bauduin P, Renoncourt A, Kopf A, Touraud D, Kunz W, Unified concept of solubilization in water by hydrotropes and cosolvents. *Langmuir* 2005; **21**: 6769–6775.
64. Balasubramanian D, Srinivas V, Gaikar VG, Sharma MM, Aggregation behavior of hydrotropic compounds in aqueous solution. *J Phys Chem B* 1989; **93**: 3865–3870.
65. Neumann MG, Schmitt CC, Prieto KR, Goi BE, The photophysical determination of the minimum hydrotrope concentration of aromatic hydrotropes. *J Colloid Interface Sci* 2007; **315**: 810–813.
66. Sanghvi R, Evans D, Yalkowsky SH, Stacking complexation by nicotinamide: A useful way of enhancing drug solubility. *Int J Pharm* 2007; **336**: 35–41.
67. Coffman RE, Kildsig DO, Self-association of nicotinamide in aqueous solution: Light-scattering and vapor pressure osmometry studies. *J Pharm Sci* 1996; **85**: 848–853.
68. Simamora P, Alvarez JM, Yalkowsky SH, Solubilization of rapamycin. *Int J Pharm* 2001; **213**: 25–29.
69. Evstigneev MP, Evstigneev VP, Santiago AA, Davies DB, Effect of a mixture of caffeine and nicotinamide on the solubility of vitamin (B2) in aqueous solution. *Eur J Pharm Sci* 2006; **28**: 59–66.
70. Landaur J, McConnell H, A study of molecular complexes formed by aniline and aromatic nitrohydrocarbons. *J Am Chem Soc* 1952; **74**: 1221–1224.
71. Mulliken RS, Structures of complexes formed by halogen molecules with aromatic and oxygenated solvent. *J Am Chem Soc* 1950; **72**: 600–608.
72. Lawrey DMG, McConnell H, A spectroscopic study of the benzene—s-Trinitrobenzene molecular complex. *J Am Chem Soc* 1952; **74**: 6175–6177.
73. Hunter CA, Lawson KR, Perkins J, Urch CJ, Aromatic interactions. *J Chem Soc Perkin Trans* 2001; **2**: 651–669.
74. Charman WN, Lai CSC, Craik DJ, Finnin BC, Reed BL, Self-association of nicotinamide in aqueous solution: N.M.R. studies of nicotinamide and the mono- and di-methyl-substituted amide analogues. *Aust J Chem* 1993; **46**: 377–385.
75. Lee SC, Acharya G, Lee J, Park K, Hydrotropic polymers: Synthesis and characterization of polymers containing picolynicotinamide moieties. *Macromolecules* 2003; **36**: 2248–2255.
76. Rowinsky EK, Donehower RC, Paclitaxel (taxol). *N Engl J Med* 1995; **332**: 1004–1014.
77. Lee J, Lee SC, Acharya G, Chang CJ, Park K, Hydrotropic solubilization of paclitaxel: Analysis of chemical structures for hydrotropic property. *Pharm Res* 2003; **20**: 1022–1030.
78. Rasool AA, Hussain AA, Dittert LW, Solubility enhancement of some water-insoluble drugs in the presence of nicotinamide and related compounds. *J Pharm Sci* 1991; **80**: 387–393.
79. Agrawal S, Pancholi SS, Jain NK, Agrawal GP, Hydrotropic solubilization of nimesulide for parenteral administration. *Int J Pharm* 2004; **274**: 149–155.
80. Nicoli S, Zani F, Bilzi S, Bettini R, Santi P, Association of nicotinamide with parabens: Effect on solubility, partition and transdermal permeation. *Eur J Pharm Biopharm* 2008; **69**: 613–621.
81. Mansur CR, Pires RV, Gonzalez G, Lucas EF, Influence of the hydrotrope structure on the physical chemical properties of polyoxide aqueous solutions. *Langmuir* 2005; **21**: 2696–2703.
82. Huh KM, Lee SC, Cho YW, Lee J, Jeong JH, Park K, Hydrotropic polymer micelle system for delivery of paclitaxel. *J Control Release* 2005; **101**: 59–68.
83. Lee SC, Huh KM, Lee J, Cho YW, Galinsky RE, Park K, Hydrotropic polymeric micelles for enhanced paclitaxel solubility: In vitro and in vivo characterization. *Biomacromolecules* 2007; **8**: 202–208.
84. Kim S, Kim JY, Huh KM, Acharya G, Park K, Hydrotropic polymer micelles containing acrylic acid moieties for oral delivery of paclitaxel. *J Control Release* 2008; **132**: 222–229.
85. Huh KM, Min HS, Lee SC, Lee HJ, Kim S, Park K, A new hydrotropic block copolymer micelle system for aqueous solubilization of paclitaxel. *J Control Release* 2008; **126**: 122–129.
86. Huang JC, Lin KT, Deanin RD, Three-dimensional solubility parameters of poly(ϵ -caprolactone). *J Appl Polym Sci* 2006; **100**: 2002–2009.
87. Nair R, Nyamweya N, Gonen S, Martinez-Miranda LJ, Hoag SW, Influence of various drugs on the glass transition temperature of poly(vinylpyrrolidone): A thermodynamic and spectroscopic investigation. *Int J Pharm* 2001; **225**: 83–96.
88. Mokrushina L, Buggert M, Smirnova I, Arlt W, Schomcker R, COSMO-RS and UNIFAC in prediction of micelle/water partition coefficients. *Ind Eng Chem Res* 2007; **46**: 6501–6509.
89. Hansch C, Quinlan JE, Lawrence GL, The linear free-energy relationship between partition coefficients and the aqueous solubility of organic liquids. *J Org Chem* 1968; **33**: 347–350.
90. Yalkowsky SH, Valvani SC, Solubility and partitioning. I: Solubility of nonelectrolytes in water. *J Pharm Sci* 1980; **69**: 912–922.

91. Yalkowsky SH, He Y, *Handbook of Aqueous Solubility Data* (CRC Press, New York, 2003).
92. Quina FH, Alonso EO, Farah JPS, Incorporation of nonionic solutes into aqueous micelles: A linear solvation free energy relationship analysis. *J Phys Chem* 1995; **99**: 11708–11714.
93. Abraham MH, Chadha HS, Dixon JP, Rafols C, Treiner C, Hydrogen bonding. Part 41. Factors that influence the distribution of solutes between water and hexadecylpyridinium chloride micelles. *J Chem Soc Perkin Trans* 1997; **2**: 19–24.
94. Rodrigues MA, Alonso EO, Yihwa C, Farah JPS, Quina FH, A linear solvent free energy relationship analysis of solubilization in mixed cationic-nonionic micelles. *Langmuir* 1999; **15**: 6770–6774.
95. Kamlet MJ, Taft RW, Solvatochromic comparison method. 1. Beta-scale of solvent hydrogen-bond acceptor (Hba) basicities. *J Am Chem Soc* 1976; **98**: 377–383.
96. Taft RW, Kamlet MJ, Solvatochromic comparison method. 2. Alpha-scale of solvent hydrogen-bond donor (Hbd) acidities. *J Am Chem Soc* 1976; **98**: 2886–2894.
97. Yokoyama T, Taft RW, Kamlet MJ, Solvatochromic comparison method. 3. Hydrogen-bonding by some 2-nitroaniline derivatives. *J Am Chem Soc* 1976; **98**: 3233–3237.
98. Kamlet MJ, Abboud JL, Taft RW, Solvatochromic comparison method. 6. Pi-star scale of solvent polarities. *J Am Chem Soc* 1977; **99**: 6027–6038.
99. Kim IW, Jang MD, Ryu YK, Cho EH, Lee YK, Park JH, Dipolarity, hydrogen-bond basicity and hydrogen-bond acidity of aqueous poly(ethylene glycol) solutions. *Anal Sci* 2002; **18**: 1357–1360.
100. Nyrkova IA, Semenov AN, Multimerization: Closed or open association model? *Eur Phys J E* 2005; **17**: 327–337.
101. Croy SR, Kwon GS, Polymeric micelles for drug delivery. *Curr Pharm Des* 2006; **12**: 4669–4684.
102. Liu R, Dannenfelser RM, Li S, in *Water-Insoluble Drug Formulation*. R. Liu (Ed.) (CRC Press, Taylor & Francis Group, New York, 2008).
103. Attwood D, Booth C, Yeates SG, Chaibundit C, Ricardo NM, Block copolymers for drug solubilisation: Relative hydrophobicities of polyether and polyester micelle-core-forming blocks. *Int J Pharm* 2007; **345**: 35–41.
104. Yamamoto Y, Yasugi K, Harada A, Nagasaki Y, Kataoka K, Temperature-related change in the properties relevant to drug delivery of poly(ethylene glycol)–poly(D,L-lactide) block copolymer micelles in aqueous milieu. *J Control Release* 2002; **82**: 359–371.
105. Marques CM, Bunchy micelles. *Langmuir* 1997; **13**: 1430–1433.
106. Allen C, Maysinger D, Eisenberg A, Nano-engineering block copolymer aggregates for drug delivery. *Adv Drug Deliv Rev* 1999; **16**: 3–27.
107. Gaucher G, Dufresne MH, Sant VP, Kang N, Maysinger D, Leroux JC, Block copolymer micelles: Preparation, characterization and application in drug delivery. *J Control Release* 2005; **109**: 169–188.
108. Kissel T, Li Y, Unger F, ABA-triblock copolymers from biodegradable polyester A-blocks and hydrophilic poly(ethylene oxide) B-blocks as a candidate for in situ forming hydrogel delivery systems for proteins. *Adv Drug Deliv Rev* 2002; **54**: 99–134.
109. Lan P, Jia L, Thermal properties of copoly(L-lactic acid/glycolic acid) by direct melt polycondensation. *J Macromol Sci Pure Appl Chem* 2006; **43**: 1887–1894.
110. Letchford K, Burt H, A review of the formation and classification of amphiphilic block copolymer nanoparticulate structures: Micelles, nanospheres, nanocapsules and polymersomes. *Eur J Pharm Biopharm* 2007; **65**: 259–269.
111. Pasquali RC, Taurozzi MP, Bregni C, Some considerations about the hydrophilic-lipophilic balance system. *Int J Pharm* 2008; **356**: 44–51.
112. Ahmed F, Pakunlu RI, Brannan A, Bates F, Minko T, Discher DE, Biodegradable polymersomes loaded with both paclitaxel and doxorubicin permeate and shrink tumors, inducing apoptosis in proportion to accumulated drug. *J Control Release* 2006; **116**: 150–158.
113. Discher DE, Ahmed F, Polymersomes. *Annu Rev Biomed Eng* 2006; **8**: 323–341.
114. Geng Y, Dalhaimer P, Cai S, Tsai R, Tewari M, Minko T, Discher DE, Shape effects of filaments versus spherical particles in flow and drug delivery. *Nat Nanotechnol* 2007; **2**: 249–255.
115. Aniansson EAG, Wall SN, On the kinetics of step-wise micelle association. *J Phys Chem* 1974; **78**: 1024–1030.
116. Halperin A, Alexander S, Polymer micelles: The relaxation kinetics. *Macromolecules* 1989; **22**: 2403–2412.
117. Prochazka K, Bednar B, Mukhtar E, Svoboda P, Trnena J, Almgren M, Nonradiative energy transfer in block copolymer micelles. *Macromolecules* 1991; **95**: 4563–4568.
118. Wang Y, Kausch CM, Chun M, Quirk RP, Mattice WL, Exchange of chains between micelles labeled polystyrene-block-poly(oxyethylene) as monitored by nonradiative single energy transfer. *Macromolecules* 1995; **28**: 904–911.

119. Haliloglu T, Bahar I, Erman B, Mattice WL, Mechanisms of the exchange of diblock copolymers between dynamic equilibrium. *Macromolecules* 1996; **29**: 4764–4771.
120. Berney C, Danuser G, FRET or no FRET: A quantitative comparison. *Biophys J* 2003; **84**: 3992–4010.
121. Prochazka K, Bednar B, Mukhtar E, Svoboda P, Trnena J, Almgren M, Nonradiative energy-transfer in block copolymer micelles. *J Phys Chem* 1991; **95**: 4563–4568.
122. Nyrkova IA, Semenov AN, On the theory of micellization kinetics. *Macromol Theory Simul* 2005; **14**: 569–585.
123. Senichev VY, Tereshatov VV, in *Handbook of Plasticizers*. G. Wypych (Ed.), (William Andrew Publishing, Norwich, NY, 2004), pp. 218–227.
124. Blasi P, Schoubben A, Giovagnoli S, Perioli L, Ricci M, Rossi C, Ketoprofen poly(lactide-co-glycolide) physical interaction. *AAPS Pharm Sci Tech* 2007; **8**: Article 37.
125. Yang X, Zhu B, Dong T, Pan P, Shuai X, Inoue Y, Interactions between an anticancer drug and polymeric micelles based on biodegradable polyesters. *Macromol Biosci* 2008; **8**: 1116–1125.
126. Liu SQ, Tong YW, Yang YY, Thermally sensitive micelles self-assembled from poly(*N*-isopropylacrylamide-co-*N,N*-dimethylacrylamide)-*b*-poly(D,L-lactide-co-glycolide) for controlled delivery of paclitaxel. *Mol Biosyst* 2005; **1**: 158–165.
127. Chen H, Kim S, He W, Wang H, Low PS, Park K, Cheng JX, Fast release of lipophilic agents from circulating PEG-PDLLA micelles revealed by in vivo Forster resonance energy transfer imaging. *Langmuir* 2008; **24**: 5213–5217.
128. Lu RC, Cao AN, Lai LH, Zhu BY, Zhao GX, Xiao JX, Interaction between bovine serum albumin and equimolarly mixed cationic-anionic surfactants decyltriethylammonium bromide-sodium decyl sulfonate. *Colloids Surf B Biointerfaces* 2005; **41**: 139–143.
129. Pi Y, Shang Y, Peng C, Liu H, Hu Y, Jiang J, Interactions between bovine serum albumin and gemini surfactant alkanediyl-alpha, omega-bis(dimethyl)decyl-ammonium bromide). *Biopolymers* 2006; **83**: 243–249.
130. Moore PN, Puvvada S, Blackshtein D, Role of the surfactant polar head structure in protein-surfactant complexation: Zein protein solubilization by SDS and by SDS/C12En surfactant solutions. *Langmuir* 2003; **19**: 1009–1016.
131. Asadi A, Saboury AA, Moosavi-Movahedi AA, Divsalar A, Sarbolouki MN, Interaction of bovine serum albumin with some novel PEG-containing diblock copolymers. *Int J Biol Macromol* 2008; **43**: 262–270.
132. Castelletto V, Krysmann M, Kelarakis A, Jauregi P, Complex formation of bovine serum albumin with a poly(ethylene glycol) lipid conjugate. *Biomacromolecules* 2007; **8**: 2244–2249.
133. Kelarakis A, Castelletto V, Krysmann MJ, Havredaki V, Viras K, Hamley IW, Interactions of bovine serum albumin with ethylene oxide/butylene oxide copolymers in aqueous solution. *Biomacromolecules* 2008; **9**: 1366–1371.
134. Ratner BD, Hoffman A, Schoen F, Lemons J, *Biomaterials Science: An Introduction to Materials in Medicine*, 2nd edn. (Academic Press, New York, 2004).
135. Amiconi G, Bonaventura C, Bonaventura J, Antonini E, Functional properties of normal and sickle cell hemoglobins in polyethylene glycol 6000. *Biochim Biophys Acta* 1977; **495**: 279–286.
136. McPherson A, Jr., Crystallization of proteins from polyethylene glycol. *J Biol Chem* 1976; **251**: 6300–6303.
137. Lee JC, Lee LL, Preferential solvent interactions between proteins and polyethylene glycols. *J Biol Chem* 1981; **256**: 625–631.
138. Rito-Palomares M, Practical application of aqueous two-phase partition to process development for the recovery of biological products. *J Chromatogr B Analyt Technol Biomed Life Sci* 2004; **807**: 3–11.
139. Rixman MA, Dean D, Ortiz C, Nanoscale intermolecular interactions between human serum albumin and low grafting density surfaces of poly(ethylene oxide). *Langmuir* 2003; **19**: 9357–9372.
140. Xia JL, Dubin PL, Kokufuta E, Dynamic and electrophoretic light-scattering of a water-soluble complex formed between pepsin and poly(ethylene glycol). *Macromolecules* 1993; **26**: 6688–6690.
141. Topchieva IN, Sorokina EM, Efremova NV, Ksenofontov AL, Kurganov BI, Noncovalent adducts of poly(ethylene glycols) with proteins. *Bioconj Chem* 2000; **11**: 22–29.
142. Furness EL, Ross A, Davis TP, King GC, A hydrophobic interaction site for lysozyme binding to polyethylene glycol and model contact lens polymers. *Biomaterials* 1998; **19**: 1361–1369.
143. Chia D, Barnett EV, Yamagata J, Knutson D, Restivo C, Furst D, Quantitation and characterization of soluble immune complexes precipitated from sera by polyethylene glycol (PEG). *Clin Exp Immunol* 1979; **37**: 399–407.

144. Herbert KE, Coppock JS, Griffiths AM, Williams A, Robinson MW, Scott DL, Fibronectin and immune complexes in rheumatic diseases. *Ann Rheum Dis* 1987; **46**: 734–740.
145. Robinson MW, Scott DG, Bacon PA, Walton KW, Coppock JS, Scott DL, What proteins are present in polyethylene glycol precipitates from rheumatic sera? *Ann Rheum Dis* 1989; **48**: 496–501.
146. Cocks DL, Wang HJ, Chen JJ, Interaction between poly(ethylene glycol) and human serum albumin. *Chem Commun* 1997; 2331–2332.
147. Pico G, Bassani G, Farruggia B, Nerli B, Calorimetric investigation of the protein-flexible chain polymer interactions and its relationship with protein partition in aqueous two-phase systems. *Int J Biol Macromol* 2007; **40**: 268–275.
148. Ragi C, Sedaghat-Herati MR, Ouameur AA, Tajmir-Riahi HA, The effects of poly(ethylene glycol) on the solution structure of human serum albumin. *Biopolymers* 2005; **78**: 231–236.
149. Hasek J, Poly(ethylene glycol) interactions with proteins. *Zeitschrift Fur Kristallographie* 2006; 613–618.
150. Baier RE, Surface behaviour of biomaterials: The theta surface for biocompatibility. *J Mater Sci Mater Med* 2006; **17**: 1057–1062.
151. Li S, Garreau H, Pauvert B, McGrath J, Toniolo A, Vert M, Enzymatic degradation of block copolymers prepared from epsilon-caprolactone and poly(ethylene glycol). *Biomacromolecules* 2002; **3**: 525–530.
152. Herzog K, Muller RJ, Deckwer WD, Mechanism and kinetics of the enzymatic hydrolysis of polyester nanoparticles by lipases. *Polym Degrad Stabil* 2006; **91**: 2486–2498.
153. Chen DR, Bei JZ, Wang SG, Polycaprolactone microparticles and their biodegradation. *Polym Degrad Stabil* 2000; **67**: 455–459.
154. Carstens MG, van Nostrum CF, Verrijck R, de Leede LG, Crommelin DJ, Hennink WE, A mechanistic study on the chemical and enzymatic degradation of PEG-oligo(epsilon-caprolactone) micelles. *J Pharm Sci* 2008; **97**: 506–518.
155. Chen C, Yu CH, Cheng YC, Yu PH, Cheung MK, Biodegradable nanoparticles of amphiphilic triblock copolymers based on poly(3-hydroxybutyrate) and poly(ethylene glycol) as drug carriers. *Biomaterials* 2006; **27**: 4804–4814.
156. Mayor S, Pagano RE, Pathways of clathrin-independent endocytosis. *Nat Rev Mol Cell Biol* 2007; **8**: 603–612.
157. Sahay G, Batrakova EV, Kabanov AV, Different internalization pathways of polymeric micelles and unimers and their effects on vesicular transport. *Bioconjug Chem* 2008; **19**: 2023–2029.
158. Edeling MA, Smith C, Owen D, Life of a clathrin coat: Insights from clathrin and AP structures. *Nat Rev Mol Cell Biol* 2006; **7**: 32–44.
159. Rappoport JZ, Focusing on clathrin-mediated endocytosis. *Biochem J* 2008; **412**: 415–423.
160. Carver LA, Schnitzer JE, Caveolae: Mining little caves for new cancer targets. *Nat Rev Cancer* 2003; **3**: 571–581.
161. Gratton SE, Ropp PA, Pohlhaus PD, Luft JC, Madden VJ, Napier ME, DeSimone JM, The effect of particle design on cellular internalization pathways. *Proc Natl Acad Sci USA* 2008; **105**: 11613–11618.
162. Chen H, Kim S, Li L, Wang S, Park K, Cheng JX, Release of hydrophobic molecules from polymer micelles into cell membranes revealed by Forster resonance energy transfer imaging. *Proc Natl Acad Sci USA* 2008; **105**: 6596–6601.
163. Miller DW, Batrakova EV, Waltner TO, Alakhov V, Kabanov AV, Interactions of pluronic block copolymers with brain microvessel endothelial cells: Evidence of two potential pathways for drug absorption. *Bioconjug Chem* 1997; **8**: 649–657.
164. Rapoport N, Marin A, Luo Y, Prestwich GD, Muniruzzaman MD, Intracellular uptake and trafficking of pluronic micelles in drug-sensitive and MDR cells: Effect on the intracellular drug localization. *J Pharm Sci* 2002; **91**: 157–170.
165. Batrakova EV, Li S, Alakhov VY, Miller DW, Kabanov AV, Optimal structure requirements for pluronic block copolymers in modifying P-glycoprotein drug efflux transporter activity in bovine brain microvessel endothelial cells. *J Pharmacol Exp Ther* 2003; **304**: 845–854.
166. Zastre JA, Jackson JK, Wong W, Burt HM, P-glycoprotein efflux inhibition by amphiphilic diblock copolymers: Relationship between copolymer concentration and substrate hydrophobicity. *Mol Pharm* 2008; **5**: 643–653.
167. Allen C, Yu Y, Eisenberg A, Maysinger D, Cellular internalization of PCL(20)-b-PEO(44) block copolymer micelles. *Biochim Biophys Acta* 1999; **1421**: 32–38.
168. Luo L, Tam J, Maysinger D, Eisenberg A, Cellular internalization of poly(ethylene oxide)-b-poly(epsilon-caprolactone) diblock copolymer micelles. *Bioconjug Chem* 2002; **13**: 1259–1265.

169. Savic R, Luo L, Eisenberg A, Maysinger D, Micellar nanocontainers distribute to defined cytoplasmic organelles. *Science* 2003; **300**: 615–618.
170. Moghimi SM, Hunter AC, Murray JC, Szewczyk A, Cellular distribution of nonionic micelles. *Science* 2004; **303**: 626–628.
171. Maysinger D, Berezovska O, Savic R, Soo PL, Eisenberg A, Block copolymers modify the internalization of micelle-incorporated probes into neural cells. *Biochim Biophys Acta* 2001; **1539**: 205–217.
172. Mahmud A, Lavasanifar A, The effect of block copolymer structure on the internalization of polymeric micelles by human breast cancer cells. *Colloids Surf B Biointerfaces* 2005; **45**: 82–89.
173. Lee RC, River LP, Pan FS, Ji L, Wollmann RL, Surfactant-induced sealing of electroporated skeletal muscle membranes in vivo. *Proc Natl Acad Sci USA* 1992; **89**: 4524–4528.
174. Collins JM, Despa F, Lee RC, Structural and functional recovery of electroporated skeletal muscle in-vivo after treatment with surfactant poloxamer 188. *Biochim Biophys Acta* 2007; **1768**: 1238–1246.
175. Maskarinec SA, Wu G, Lee KY, Membrane sealing by polymers. *Ann NY Acad Sci* 2005; **1066**: 310–320.
176. Lentz BR, PEG as a tool to gain insight into membrane fusion. *Eur Biophys J* 2007; **36**: 315–326.
177. Blow AM, Botham GM, Fisher D, Goodall AH, Tilcock CP, Lucy JA, Water and calcium ions in cell fusion induced by poly(ethylene glycol). *FEBS Lett* 1978; **94**: 305–310.
178. Wu JR, Lentz BR, Mechanism of poly(ethylene glycol)-induced lipid transfer between phosphatidylcholine large unilamellar vesicles: A fluorescent probe study. *Biochemistry* 1991; **30**: 6780–6787.
179. Burgess SW, Massenburg D, Yates J, Lentz BR, Poly(ethylene glycol)-induced lipid mixing but not fusion between synthetic phosphatidylcholine large unilamellar vesicles. *Biochemistry* 1991; **30**: 4193–4200.
180. Talbot WA, Zheng LX, Lentz BR, Acyl chain unsaturation and vesicle curvature alter outer leaflet packing and promote poly(ethylene glycol)-mediated membrane fusion. *Biochemistry* 1997; **36**: 5827–5836.
181. Shi R, Borgens RB, Acute repair of crushed guinea pig spinal cord by polyethylene glycol. *J Neurophysiol* 1999; **81**: 2406–2414.
182. Liu-Snyder P, Logan MP, Shi R, Smith DT, Borgens RB, Neuroprotection from secondary injury by polyethylene glycol requires its internalization. *J Exp Biol* 2007; **210**: 1455–1462.
183. Batrakova EV, Li S, Li Y, Alakhov VY, Elmquist WF, Kabanov AV, Distribution kinetics of a micelle-forming block copolymer Pluronic P85. *J Control Release* 2004; **100**: 389–397.
184. Rudin M, Weissleder R, Molecular imaging in drug discovery and development. *Nat Rev Drug Discov* 2003; **2**: 123–131.
185. Torchilin VP, Micellar nanocarriers: Pharmaceutical perspectives. *Pharm Res* 2007; **24**: 1–16.
186. Wooley KL, Shell crosslinked polymer assemblies: Nanoscale constructs inspired from biological systems. *J Polym Sci A: Polym Chem* 2000; **38**: 1397–1407.
187. O'Reilly RK, Hawker CJ, Wooley KL, Cross-linked block copolymer micelles: Functional nanostructures of great potential and versatility. *Chem Soc Rev* 2006; **35**: 1068–1083.
188. Sun X, Rossin R, Turner JL, Becker ML, Joralemon MJ, Welch MJ, Wooley KL, An assessment of the effects of shell cross-linked nanoparticle size, core composition, and surface PEGylation on in vivo biodistribution. *Biomacromolecules* 2005; **6**: 2541–2554.
189. Sun G, Hagooley A, Xu J, Nystrom AM, Li Z, Rossin R, Moore DA, Wooley KL, Welch MJ, Facile, efficient approach to accomplish tunable chemistries and variable biodistributions for shell cross-linked nanoparticles. *Biomacromolecules* 2008; **9**: 1997–2006.
190. Shuai X, Merdan T, Schaper AK, Xi F, Kissel T, Core-cross-linked polymeric micelles as paclitaxel carriers. *Bioconjug Chem* 2004; **15**: 441–448.
191. Li Y, Lokitz BS, Armes SP, McCormick CL, Synthesis of reversible shell cross-linked micelles for controlled release of bioactive agents. *Macromolecules* 2006; **39**: 2726–2728.
192. Kohn J, New approaches to biomaterials design. *Nat Mater* 2004; **3**: 745–747.
193. Kohn J, Welsh WJ, Knight D, A new approach to the rationale discovery of polymeric biomaterials. *Biomaterials* 2007; **28**: 4171–4177.
194. Matyjaszewski K, Xia J, Atom transfer radical polymerization. *Chem Rev* 2001; **101**: 2921–2990.
195. Stenzel MH, RAFT polymerization: An avenue to functional polymeric micelles for drug delivery. *Chem Commun* 2008; **14**: 3486–3503.
196. Hawker CJ, Bosman AW, Harth E, New polymer synthesis by nitroxide mediated living radical polymerizations. *Chem Rev* 2001; **101**: 3661–3688.
197. Kwon IK, Kim SW, Chaterji S, Vedantham K, Park K, in *Smart Materials*, M. Schwartz (Ed.) (Taylor & Francis Group, LLC, Boca Raton, FL, 2009), pp. 11–13.
198. Hamaguchi T, Kato K, Yasui H, Morizane C, Ikeda M, Ueno H, Muro K et al., A phase I and pharmacokinetic study of NK105, a paclitaxel-incorporating micellar nanoparticle formulation. *Br J Cancer* 2007; **97**: 170–176.

AQ8

AQ9
AQ10

199. Fredrickson GH, Pincus P, Drainage of compressed polymer layers - dynamics of a squeezed sponge. *Langmuir* 1991; **7**: 786–795.
200. Yokoyama M, Okano T, Sakurai Y, Fukushima S, Okamoto K, Kataoka K, Selective delivery of adriamycin to a solid tumor using a polymeric micelle carrier system. *J Drug Target* 1999; **7**: 171–186.
201. Armstrong JK, Leharne SA, Stuart BH, Snowden MJ, Chowdhry BZ, Phase transition properties of poly(ethylene oxide) in aqueous solutions of sodium chloride. *Langmuir* 2001; **17**: 4482–4485.
202. Park YJ, Lee JY, Chang YS, Jeong JM, Chung JK, Lee MC, Park KB, Lee SJ, Radioisotope carrying polyethylene oxide-polycaprolactone copolymer micelles for targetable bone imaging. *Biomaterials* 2002; **23**: 873–879.
203. Liu J, Zeng F, Allen C, In vivo fate of unimers and micelles of a poly(ethylene glycol)-block-poly(caprolactone) copolymer in mice following intravenous administration. *Eur J Pharm Biopharm* 2007; **65**: 309–319.
204. Savic R, Azzam T, Eisenberg A, Maysinger D, Assessment of the integrity of poly(caprolactone)-*b*-poly(ethylene oxide) micelles under biological conditions: A fluorogenic-based approach. *Langmuir* 2006; **22**: 3570–3578.
205. Novakova K, Laznicek M, Rypacek F, Machova L, Pharmacokinetics and distribution of 125I-PLA-*b*-PEO block copolymers in rats. *Pharm Dev Technol* 2003; **8**: 153–161.
206. Novakova K, Laznicek M, ¹²⁵I-labeled PLA/PEO block copolymer: Biodistribution studies in rats. *J Bioact Compat Polym* 2002; **17**: 285–296.
207. Yamamoto Y, Nagasaki Y, Kato Y, Sugiyama Y, Kataoka K, Long-circulating poly(ethylene glycol)-poly(D,L-lactide) block copolymer micelles with modulated surface charge. *J Control Release* 2001; **77**: 27–38.
208. Yokoyama M, Okano T, Sakurai Y, Ekimoto H, Shibasaki C, Kataoka K, Toxicity and antitumor activity against solid tumors of micelle-forming polymeric anticancer drug and its extremely long circulation in blood. *Cancer Res* 1991; **51**: 3229–3236.
209. Sezgin Z, Yuksel N, Baykara T, Preparation and characterization of polymeric micelles for solubilization of poorly soluble anticancer drugs. *Eur J Pharm Biopharm* 2006; **64**: 261–268.

AUTHOR QUERIES

- [AQ1] Please check the phrase: “toxicity,originating” for sense in the sentence starting “Excipients...”
- [AQ2] Please check the phrase: “castor oil. iwhen” for sense in the sentence starting: “For example,.....”
- [AQ3] Please check the phrase: “the phosphatidylserine.and” for sense in the sentence starting: “The size of.....” Also, please check the phrase: “blood clearance.is used” for sense in the next sentence.
- [AQ4] Please check if the edit made to the sentence starting “Line II and III...” is OK.
- [AQ5] Please check for sense in the sentence starting “A too high DP possibly makes...”
- [AQ6] Please check the citation of reference [31] in the footnote of Table 19.7.
- [AQ7] Reference details of references [117,121] are the same except the journal title. Please check.
- [AQ8] References [113,173] are exactly one and the same. So we have deleted the repeated version and renumbered the reference list. Please check.
- [AQ9] Please check the page range of reference [198].
- [AQ10] References [198–209] have no in-text citations. Please check.

